Chimeric spike mRNA vaccines protect against sarbecovirus challenge in mice

David R. Martinez [1, *,] Alexandra Schaefer [1,] Sarah R. Leist [1], Gabriela De la Cruz [2], Ande West[1], Elena N. Atochina-Vasserman [4], Robert Parks [5], Maggie Barr [5], Dapeng Li [5], Boyd Yount [1], Kevin O. Saunders [5], Drew Weissman [4], Barton F. Haynes [5], Stephanie A. Montgomery [3], Ralph S. Baric [1, *].

[1] Department of Epidemiology, University of North Carolina at Chapel Hill, Chapel Hill, NC, USA

[2] Lineberger Comprehensive Cancer Center, University of North Carolina School of Medicine, Chapel Hill, NC, USA

[3] Department of Laboratory Medicine and Pathology, University of North Carolina School of Medicine, Chapel Hill, NC, USA

[4] Infectious Disease Division, Department of Medicine, Perelman School of Medicine, University of Pennsylvania Perelman School of Medicine, Philadelphia, PA, USA

[5] Duke Human Vaccine Institute, Duke University School of Medicine, Durham, NC, USA

[*]Corresponding authors.

David R. Martinez, D.R.M., david.rafael.martinez@gmail.com
Ralph S. Baric, R.S.B., rbaric@email.unc.edu

Keywords: SARS-CoV-2, SARS-like virus, *Sarbecovirus*, mRNA vaccine, universal coronavirus vaccine.

Abstract

The emergence of SARS-CoV and SARS-CoV-2 in the 21st century highlights the need to develop universal vaccination strategies against the SARS-related *Sarbecovirus* subgenus. Using structure-guided chimeric spike designs and multiplexed immunizations, we demonstrate protection against SARS-CoV, SARS-CoV-2, and bat CoV (BtCoV) RsSHC014 challenge in highly vulnerable aged mice. Chimeric spike mRNAs containing N-terminal domain (NTD), and

receptor binding domains (RBD) induced high levels of broadly protective neutralizing antibodies against three high-risk sarbecoviruses: SARS-CoV, RsSHC014, and WIV-1. In contrast, SARS-CoV-2 mRNA vaccination not only showed a 10 to >500-fold reduction in neutralizing titers against heterologous sarbecovirus strains, but SARS-CoV challenge in mice resulted in breakthrough infection including measurable lung pathology. Importantly, chimeric spike mRNA vaccines efficiently neutralized both the D614G and the South African B.1.351 variants of concern despite some reduction in neutralization activity. Thus, multiplexed-chimeric spikes may provide a novel strategy to prevent pandemic and SARS-like zoonotic coronavirus infections, while revealing the limited efficacy of SARS-CoV-2 spike vaccines against other sarbecoviruses.

Introduction

A novel coronavirus that caused severe acute respiratory syndrome (SARS-CoV) emerged in 2003 and caused more than 8,000 infections and ~800 deaths worldwide (*1*). Less than a decade later, another coronavirus that caused Middle East Respiratory Syndrome (MERS-CoV) emerged in Saudi Arabia in 2012 (*2*), resulting in an ongoing outbreak with at least ~2,600 cases and 900 deaths (*3*). In December 2019, another novel human SARS-like virus from the genus *Betacoronavirus* and subgenus *Sarbecocovirus* emerged in Wuhan China, designated SARS-CoV-2 (*4*, *5*). The emergence and spread of SARS-CoV-2, the causative agent of coronavirus disease 2019 (COVID-19), was explosive. By March 2020, the World Health Organization (WHO) had declared COVID-19 a global pandemic. By March 2021, more than 117 million COVID-19 human infections had resulted in more than 2.6 million deaths globally in an ever-expanding pandemic (*6*).

Zoonotic transmission of animal coronaviruses of probable bat origin into naïve animal and human populations remains a clear One Health threat (*7-10*). Broadly protective vaccines and therapeutic monoclonal antibodies are desperately needed to mitigate the risk of animal coronavirus zoonosis into naïve species including humans. Bats are known reservoirs of SARS-like coronaviruses (CoVs) and harbor high-risk "pre-emergent" SARS-like variant strains, such as WIV-1 and RsSHC014, which are able to utilize human ACE2 receptors for entry, replicate efficiently in primary airway epithelial cells, and may escape existing countermeasures (*9-13*) Given the high pandemic potential of zoonotic and epidemic sarbecoviruses (*13*), the development of broadly effective countermeasures, such as universal vaccination strategies, antibodies and drugs is a global health priority (*14-17*). However, a major hurdle to develop vaccines that can neutralize diverse sarbecoviruses is the vast genetic diversity that exists within critical immunodominant epitope landscapes, like the receptor binding domain (RBD) (*13*). As COVID-19 convalescent patients exhibit little cross-neutralization of other human pathogenic viruses including SARS-CoV and MERS-CoV (*18, 19*), it is uncertain whether natural immunity to SARS-CoV-2 will protect against other sarbecoviruses of zoonotic origin that may emerge in the future. As double-inactivated SARS-CoV vaccines in aged mice reported increased eosinophilic infiltration in the lung following heterologous sarbecovirus challenge, it is critical to examine heterologous challenge in the context of sarbecovirus vaccination (*20, 21*). This particularly important as high levels of neutralizing antibodies are required for protecting against vaccine-associated enhanced respiratory disease (VAERD) following heterologous SARS-CoV challenge in aged mice.

The RBD is a target for neutralizing antibodies elicited in the context of natural SARS-CoV-2 and MERS-CoV infections (*22-25*). In addition to the RBD, the N-terminal domain

(NTD) is also a target for SARS-CoV-2 and MERS-CoV neutralizing antibodies (*23*, *26*, *27*). Passive immunization with SARS-CoV-2 NTD-specific antibodies can protect naïve mice from challenge, demonstrating that the NTD is a target of protective immunity (*28*). However, it remains unclear if vaccine-elicited neutralizing antibodies induced by vaccines can protect against *in vivo* challenge with epidemic and bat coronaviruses. Here, we provide the proof-of-concept that nucleoside-modified mRNA-lipid nanoparticle (LNP) vaccines expressing chimeric spikes containing admixtures of RBD and NTD domains from epidemic and pandemic sarbecoviruses can: 1) elicit robust neutralizing antibody responses against multiclade sarbecoviruses, and 2) protect against viral replication in upper and lower respiratory airways of both epidemic and pandemic human coronaviruses in aged mice, and 3) attenuate VAERD responses associated with homologous virus challenge. Our findings suggest that mRNA-LNP vaccination with chimeric CoV spikes is a viable strategy to protect against contemporary and high-risk sarbecovirus emergence events.

Results

Design and expression of chimeric spike constructs to cover pandemic and zoonotic SARS-related coronaviruses

Sarbecoviruses exhibit considerable genetic diversity (Fig. 1A) and several bat CoVs (Bt-CoVs) that are SARS-like exist in nature (*13*). As previous studies have demonstrated that Bt-CoVs, including WIV-1 and RsSHC014, are poised for emergence (*9, 10*), we sought to design vaccination strategies that can protect against antigenically diverse, epidemic, pandemic, and pre-pandemic CoVs isolated from humans or *Rhinolophus* bats. Harnessing the modular design

of CoV spikes (*29*), we designed chimeric spikes to create within-spike "bivalent" and "trivalent" vaccines that have the potential to elicit protective antibody responses against more than one virus within a subgenus (e.g., *Sarbecovirus*). As the NTD and RBD are both the target of binding and neutralizing antibodies, we used domain-focused immunogen design, which admixes major neutralizing antigenic sites (e.g., NTD, RBD, S2) into new spike modules from clade I, II, and III sarbecoviruses designed to maximize breadth while focusing immunity against broadly conserved high-risk spike domains. To achieve vaccination strategies that can overcome the broad genetic diversity of SARS-like viruses, we designed four sets of chimeric spike constructs that contained unique admixtures of the RBD and/or NTD neutralizing domains from various pandemic and zoonotic SARS-like viruses. Chimera 1 included the NTD from Bt-CoV Hong Kong University 3-1 (HKU3-1), the SARS-CoV RBD, and the SARS-CoV-2 subunit 2 (S2) (Fig. S1A). Chimera 2 included SARS-CoV-2 RBD and SARS-CoV NTD and S2. Chimera 3 included the SARS-CoV RBD, SARS-CoV-2 NTD and S2. Finally, chimera 4 included the RsSHC014 RBD, SARS-CoV-2 NTD and S2. We also generated a monovalent SARS-CoV-2 spike furin knock out (KO) vaccine, partially phenocopying the Johnson & Johnson, Moderna, and Pfizer vaccines that recently received emergency use authorization by the U.S. FDA, and a negative control norovirus GII capsid vaccine (Fig. S1A to F). We generated these chimeric spikes and control spikes as lipid nanoparticle-encapsulated, nucleoside-modified mRNA (mRNA-LNP) vaccines as described previously (*30*), and verified their expression in HEK cells (Fig. S1G). To confirm that coronavirus spikes are modular in design allowing for rationale admixing of component parts, we also designed and recovered a panel of high titer recombinant live viruses between RsSHC014 nanoluciferase ΔORF7&8 that harbored motifs from the SARS-CoV-2 S1, NTD, RBD and S2 domains. After infection *in vitro*, these high-titer recombinant

129 viruses expressed high levels of nanoluciferase, demonstrating that the chimeric spikes promoted
130 efficient entry and replication (Fig. S1H).
131
132 **Immunogenicity of mRNAs expressing chimeric spike constructs against coronaviruses**
133 As previous studies demonstrated the successful delivery of more than one HSV-2
134 glycoprotein to broaden antigen coverage via mRNA vaccination (*31*-*33*), we sought to
135 determine if simultaneous immunization with mRNA-LNP expressing the chimeric spikes of
136 diverse sarbecoviruses was a feasible strategy to elicit broadly binding and neutralizing
137 antibodies. As aged human populations are the most susceptible to severe COVID-19 disease and
138 death, we sought to examine the protective efficacy of our vaccines in aged mouse models that
139 develop severe disease and death following sarbecovirus infection. We immunized aged mice
140 with the chimeric spikes formulated to induce cross reactive responses to the NTD and RBD
141 against multiple divergent clade I-III sarbecoviruses, and/or focused boosting of antibody
142 responses against epidemic strains, a SARS-CoV-2 furin KO spike, and a GII.4 norovirus capsid
143 negative control. Group 1 was primed and boosted with chimeric spikes 1, 2, 3, and 4 (Fig. 1B).
144 Group 2 was primed with chimeric spikes 1 and 2 and boosted with chimeric spikes 3 and 4.
145 Group 3 was primed and boosted with chimeric spike 4. Group 4 was primed and boosted with
146 the monovalent SARS-CoV-2 furin knockout spike. Finally, group 5 was primed and boosted
147 with a norovirus capsid GII.4 Sydney 2011 strain (Fig. 1B). To examine the magnitude and cross
148 binding responses of the chimeric spikes compared to the SARS-CoV-2 monovalent vaccine, we
149 examined the binding antibody responses by ELISA against a diverse panel of CoV spike
150 proteins that included contemporary, epidemic, pandemic, and zoonotic coronaviruses. While
151 pre-immunization mouse serum samples did not bind to any of the coronavirus ELISA panel

antigens, we observed high binding to SARS-CoV-2 and SARS-like spike antigens in several of the vaccinated groups (Fig 2 and Fig. S2). Mice immunized with chimeric spikes 1-4 either in combination or separately in the prime/boost generated the highest magnitude responses to SARS-CoV Toronto Canada isolate (Tor2) and HKU3-1 spike compared to mice immunized with chimera 4 and a SARS-CoV-2 furin KO spike (Fig 2A and 2H), demonstrating that immunization with multiplexed chimeric spikes elicits higher magnitude and more cross-reactive antibody profiles than immunization with a monovalent SARS-CoV-2 spike mRNA-LNP. While mice primed with chimeras 1-2 and boosted with chimeras 3-4 generated lower magnitude binding responses to both SARS-CoV-2 RBD (Fig. 2C) and SARS-CoV-2 NTD (Fig 2D), mice immunized with chimeras 1-4 in the prime and boost generated similar magnitude binding antibodies to SARS-CoV-2 D614G compared to mice immunized with the SARS-CoV-2 furin KO spike mRNA-LNP (Fig 2B). Mice immunized with the chimeric spikes 1-4 all together or separately in the prime and boost generated similar magnitude binding antibody responses against SARS-CoV-2 D614G, Pangolin GXP4L, and RaTG13 spikes (Fig. 2B, 2E, and 2F) compared to mice immunized with SARS-CoV-2 spike, underlining that the chimeric spikes not only generate indistinguishable binding responses against SARS-CoV-2-like viruses compared to monovalent SARS-CoV-2 vaccines but also elicit higher responses against SARS-like viruses at high risk of emergence. Mice immunized with chimeras 1-4 in the prime and boost generated the highest magnitude binding antibodies to RsSHC014 spike (Fig. 2G). Importantly, mice immunized with the norovirus capsid mRNA-LNP vaccine did not generate binding IgG antibodies to any of the tested CoV protein antigens (Fig 2 and Fig. S2). In agreement with the binding ELISA data, mice immunized with chimeras 1-4 in the prime and boost elicited indistinguishable magnitude levels of hACE2 blocking responses to the SARS-CoV-2 spike

175 immunized mice (Fig. 2J). In contrast, mice from groups 2 and 3 elicited lower magnitude
176 blocking responses against hACE2 compared to mice from groups 1 and 4 (Fig. 2J). Finally, we
177 did not observe cross-binding antibodies against common-cold CoV spike antigens from HCoV-
178 HKU1, HCoV-NL63, and HCoV-229E, in most of the vaccine groups (Fig. S2A-2D), but we did
179 observe low binding levels against more distant group 2C MERS-CoV (Fig. 2I) and
180 Betacoronaviruses like group 2A HCoV-OC43 in vaccinated mice from groups 1 and 2 (Fig.
181 S2B). Altogether, these results suggest that chimeric spike mRNA vaccines elicit more broad and
182 higher magnitude binding responses against pandemic and bat SARS-like viruses compared to
183 monovalent SARS-CoV-2 spike furin KO mRNA-LNP vaccines.
184
185 **Neutralizing antibody responses against live sarbecoviruses and variants of concern**
186 We then tested the neutralizing antibody responses against SARS-CoV, SARS-CoV-2,
187 Bt-CoV RsSHC014, and BtCoV WIV-1, using live viruses expressing nanoluciferase as
188 previously described (Fig 3A-3D) (*18*). Group 4 SARS-CoV-2 S mRNA vaccinated animals
189 mounted a robust response against SARS-CoV-2, however responses against SARS-CoV,
190 RsSHC014, and WIV-1 were 18-, >500- or 116-fold more resistant, respectively, demonstrating
191 the importance of including different high-risk pre-emergent Bt-sarbecovirus strains in these
192 studies (Fig 3A-3D and Fig. S3G-H). In contrast, aged mice that were primed with chimeras 1-2
193 and boosted with chimeras 3-4 showed a 42- and 2-fold increase in neutralizing titer against
194 SARS-CoV and WIV1, and less than 1-fold decrease against RsSHC014 relative to SARS-CoV-
195 2 neutralizing titers (Fig 3A-3D and Fig. S3C-D). The chimera 4 vaccine, which contained the
196 RsSHC014 RBD/SARS-CoV-2 NTD and S2 domains, elicited 3-, 7-fold higher neutralizing
197 titers against SARS-CoV and RsSHC014 yet showed a 3-fold reduction in WIV-1 neutralizing

198 titers relative to its SARS-CoV-2 neutralizing activity (Fig 3A-3D and Fig. S3E-F). Finally, mice
199 immunized with chimeras 1-4 as prime and boost together generated the most balanced and
200 highest neutralizing titers that were 13- and 1.2-fold higher against SARS-CoV and WIV-1 and
201 only less than 1-fold lower against RsSHC014 relative to the SARS-CoV-2 neutralizing titers in
202 this group (Fig 3A-3D and Fig. S3A-B). We also examined the neutralizing activity of mice
203 primed and boosted with chimeras 1-4 vs. the monovalent SARS-CoV-2 vaccine against two
204 variants of concern (VOC): the predominant D614G variant and the B.1.351 South African
205 variant. The serum of aged mice immunized with the multiplexed chimeras and the monovalent
206 SARS-CoV-2 vaccine neutralized the dominant D614G variant with similar potency as the wild
207 type D614 non-predominant variant (Fig. 3E). Mouse sera from group 1 primed and boosted with
208 chimeras 1-4 only had a 2-fold reduction in neutralizing activity against the B.1.351 South
209 African variant of concern, whereas a 4-fold reduction was observed in the SARS-CoV-2 furin
210 KO immunized mouse sera (Fig. 3F). Despite the significant but small reduction in neutralizing
211 activity against the B.1.351 variant, we did not observe a complete ablation in neutralizing
212 activity in either group. Thus, both monovalent SARS-CoV-2 vaccines and multiplexed chimeric
213 spikes elicit neutralizing antibodies against newly emerged SARS-CoV-2 variants and
214 multiplexed chimeric spike vaccines outperform the monovalent SARS-CoV-2 vaccines in terms
215 of breadth of potency against multiclade sarbecoviruses.
216
217 ***In vivo* protection against epidemic and pandemic coronavirus challenge**
218 To assess the ability of the mRNA-LNP vaccines in mediating protection against
219 previously epidemic SARS-CoV, pandemic SARS-CoV-2, and Bt-CoVs, we challenged the
220 different groups and observed the mice for signs of clinical disease. Group 1 mice (chimeras 1-4

prime/boost) or group 2 (chimeras 1-2 prime, 3-4 boost) were completely protected from weight loss, lower, and upper airway virus replication as measured by infectious virus plaque assays following SARS-CoV mouse-adapted (MA15) challenge (Fig. 4A, 4B and 4C). Similarly, these two vaccine groups were also protected against SARS-CoV-2 mouse-adapted (MA10). In contrast, groups 3 (chimera 4) showed some protection against SARS-CoV MA15 induced weight loss, but not against viral replication in the lung or nasal turbinates, and full protection against SARS-CoV-2 MA10. In contrast, norovirus capsid control mice developed severe disease including mortality in both SARS-CoV MA15 and SARS-CoV-2 MA10 infections (Fig. S5). Monovalent SARS-CoV-2 mRNA vaccines were highly efficacious against SARS-CoV-2 MA10 challenge but failed to protect against SARS-CoV MA15-induced weight loss, and replication in the lower and upper airway (Fig. 4A, 4B, and 4C), suggesting that SARS-CoV-2 mRNA-LNP vaccines currently being administered during the COVID-19 pandemic are not likely to protect against future SARS-CoV emergence events in vulnerable populations. Mice from all chimeric spike immunization groups, including group 4 which received the SARS-CoV-2 NTD/RsSHC014 RBD chimeric spike, and SARS-CoV-2 furin KO vaccine groups were completely protected from weight loss and lower airway SARS-CoV-2 MA10 replication (Fig. 4D, 4E, and 4F). In addition, using the BtCoV RsSHC014 replication model in mice, we also demonstrated protection against RsSHC014 replication in the lung and nasal turbinates (Fig. S4) in mice that received the multiplexed chimeras 1-4 as prime and boost and in mice that immunized with the SARS-CoV-2 NTD/RsSHC014 RBD chimeric spike, demonstrating the breadth of the universal spike vaccine formulations and the ability to introduce “bivalency” into CoV spike to increase protection. Our findings also suggest that SARS-CoV-2 mRNA-LNP vaccines do not protect against clinical disease of SARS-CoV MA15 infection in mice.

Lung pathology and cytokines in mRNA-LNP vaccinated mice challenged with epidemic and pandemic coronaviruses

Lung discoloration is the gross manifestation of various processes of acute lung damage, including congestion, edema, hyperemia, inflammation, and protein exudation. We used this macroscopic scoring scheme to visually score mouse lungs at the time of harvest. To quantify the pathological features of acute lung injury (ALI) in mice, we used a tool from the American Thoracic Society (ATS - Matute-Bello lung pathology score). We have previously used this tool to describe the pulmonary pathogenesis in BALB/c mice infected with SARS-CoV-2 MA10 (*34, 35*). To quantify microscopic differences in lung pathology, we used this tool on three random diseased fields in lung tissue sections per mouse and tissues were blindly evaluated by a board-certified veterinary pathologist (Fig. 5B). With a complementary histological quantitation tool, we similarly scored lung tissue sections for diffuse alveolar damage (DAD), the pathological hallmark of ALI (cellular sloughing, necrosis, hyaline membranes, etc.) (*36*, *37*) and found these data were generally consistent with those from the lung discoloration scores. We observed significant lung pathology by both the Matute-Bello and DAD scoring tools in groups 4 and 5 vaccinated animals, consistent with the weight loss, lung titer, and lung cytokine data after heterologous SARS-CoV MA15 challenge. In contrast, multiplexed chimeric spike vaccine formulations in groups 1 and 2 provided complete protection from lung pathology after SARS-CoV MA15 challenge (Fig. 5A and 5B). Concerningly, mice immunized with the SARS-CoV-2 spike that showed breakthrough infection with SARS-CoV MA15 developed severe lung inflammation, potentially suggesting that future outbreaks of SARS-CoV may lead to lung pathology in individuals vaccinated with SARS-CoV-2. In contrast to the heterologous SARS-

CoV MA15 challenge, all groups challenged with SARS-CoV-2 MA10 were protected against lung pathology compared to the norovirus capsid-immunized control group. Mice immunized with the multiplexed chimeric spikes alone or in combination, and also with the SARS-CoV-2 NTD/RsSHC014 chimera, and with SARS-CoV-2 were also completely protected against both macroscopic and microscopic lung damage (Fig 5C and 5D).

To examine the level of protection in the lung of SARS-CoV and SARS-CoV-2 challenged mice in more detail, we measured lung proinflammatory cytokines and chemokines in the different vaccination groups. Group 1 mice (chimeras 1-4 prime/boost) and group 2 (chimeras 1-2 prime, 3-4 boost) mice following SARS-CoV MA15 challenge had baseline levels of macrophage activating cytokines and chemokines including, IL-6, CCL2, IL-1α, G-SCF, and CCL4, compared to group 5 (norovirus prime/boost) (Fig. S6A). In contrast, group 3 (chimera 4 prime/boost) and group 4 (monovalent SARS-CoV-2 prime/boost) mice following SARS-CoV MA15 challenge, showed high and indistinguishable levels of IL-6, CCL2, IL-1α, G-SCF, and CCL4 compared to group 5. Following SARS-CoV-2 MA10 challenge, group 4 and group 1 showed the lowest levels of IL-6, and G-SCF relative to group 5 controls (Fig. S6B), and we only observed significant reductions in CCL2, IL-1α, CCL4 lung levels in groups 3 and 4 compared to the group 5 control despite full protection from weight loss, lower, and some level of upper airway replication in groups 1-4. These results suggest that SARS-CoV-2 vaccination does not protect against SARS-CoV challenge and underlines that universal vaccination strategies that can protect against heterologous sarbecovirus strains at high risk for human emergence are needed.

Discussion

The mRNA-1273 vaccine developed by Moderna Inc. demonstrated protection against SARS-CoV-2 challenge both in mice and in non-human primates (*38*, *39*), but there is a growing concern due to the emergence of VOCs like South African B1.351 which is 2-6 fold more resistant to vaccine-elicited polyclonal neutralizing antibodies (*40*). Both the Moderna and Pfizer/BioNTech mRNA-LNP vaccines were safe and efficacious against SARS-CoV-2 infections in large Phase 3 efficacy human clinical trials (*41-43*), and the Moderna mRNA-1273 vaccine was also immunogenic in aged adults (*44*), which are highly vulnerable for severe COVID-19 symptoms and death. Given the rapid development and success of the mRNA-LNP vaccine platform, we sought to replicate this existing platform to establish the proof-of-concept of vaccine protection against sarbecoviruses in aged mouse models that recapitulate extreme vulnerability of aged human populations. Consistent with previous studies that measured efficacy of mRNA-LNP vaccines for SARS-CoV-2 vaccines in mice (*38*), our monovalent SARS-CoV-2 vaccine elicited robust neutralizing antibody titers to the SARS-CoV-2 D614G variant. We observed a 2-fold reduction in neutralizing antibodies in mice immunized with the multiplexed-chimeric spikes and a 4-fold reduction in neutralizing antibodies in SARS-CoV-2 monovalent vaccinated mice against the South African B.1.351 VOC. While monovalent SARS-CoV-2 vaccinated mice showed an 18 to >500-fold reduction in neutralization antibody activity against clade I and clade III sarbecoviruses, multiplexed chimeric spike immunizations showed improved neutralizing antibody activity against these epidemic and zoonotic sarbecoviruses (Fig. 3 and Fig. S3). The lack of protection against SARS-CoV challenge in SARS-CoV-2 immunized mice underlines the need for the development of universal vaccination strategies that can achieve broader coverage against pre-emergent bat SARS-CoV-like and SARS-CoV-2-like viruses. One

such strategy, as described herein, is to admix key antigenic sites (e.g., NTD and RBD) from different sarbecoviruses into new chimeric spikes that are designed to enhance breadth while focusing the neutralization responses on key antigenic sites conserved across multiple strains (e.g. S2). A caveat of including multiple chimeric spikes in a single shot is the potential formation of heterotrimers not present in the intended vaccine formulation. While it remains unknown if our chimeric mRNA-LNP vaccines generate heterotrimers *in vivo*, the robustness of the cross-neutralizing titers against sarbecoviruses and protection against SARS-CoV and SARS-CoV-2 in groups 1 and 2 in aged mice lends support to this strategy as a way to elicit broadly cross-reactive neutralizing antibodies against Group 2B coronaviruses. In agreement with this notion, chimera 4, which contains the RsSHC014 RBD and SARS-CoV-2 NTD and S2, elicited binding and neutralizing antibodies and also fully protected mice from BtCoV RsSHC014 and SARS-CoV-2 challenge, suggesting that CoV spikes vaccines can be designed to maximize their display of neutralizing and protective epitopes that can cover more than one pandemic/epidemic/pre-emergent CoV that are at high risk for emergence into naïve human populations. While other strategies also exist, such as multiplexing mosaic sarbecovirus RBDs (*19*), S1 or spike glycoproteins and RBDs on nanoparticles (*45*), chimeric spike mRNA-LNP vaccination can clearly achieve broad protection, using existing manufacturing technologies, and are highly portable to other high-risk emerging coronaviruses like group 2C MERS-CoV-related strains. It is notable that our chimeric spike vaccines and the SARS-CoV-2 furin KO, all of which lacked the two proline stabilizing mutations (S-2P) vaccines protected aged mice from challenge. This suggests that the two proline stabilization mutations (S2P) are not required for eliciting protective levels of neutralizing antibodies in aged mice, although such mutations may enhance the neutralization titers after immunization (*38, 46*).

As previously reported with RNA recombinant viruses, our chimeric spike live viruses containing SARS-CoV-2 antigenic domains not only demonstrate the known interchangeability and functional plasticity of CoV spike glycoprotein structural motifs (*29*, *47*, *48*), but also could serve as live-attenuated vaccines. Our demonstration of cross-protection against sarbecoviruses in mice lends support to the notion that universal vaccines against group 2B CoVs is likely achievable. Moving forward it will be important to determine if these chimeric mRNA-LNP vaccines can also protect in large pre-clinical animal models, such as rhesus macaques, and if the S2P mutations will improve the novel chimeric spikes described herein. We conclude that chimeric mRNA spikes vaccines comprised of zoonotic, epidemic, and pandemic coronaviruses are a feasible strategy to protect against high-risk, pre-emergent, and pandemic sarbecovirus infections.

Methods

Chimeric spike vaccine design and formulation

Chimeric spike vaccines were designed with RBD and NTD swaps to increase coverage of epidemic (SARS-CoV), pandemic (SARS-CoV-2), and high-risk pre-emergent bat CoVs (bat SARS-like HKU3-1, and bat SARS-like RsSHC014). Chimeric and monovalent spike mRNA-LNP vaccines were designed based on SARS-CoV-2 spike (S) protein sequence (Wuhan-Hu-1, GenBank: MN908947.3), SARS-CoV (urbani GenBank: AY278741), bat SARS-like CoV HKU3-1 (GenBank: DQ022305), and Bat SARS-like RsSHC014 (GenBank: KC881005). Coding sequences of full-length SARS-CoV-2 furin knockout (RRAR furin cleavage site abolished between amino acids 682-685), the four chimeric spikes, and the norovirus capsid negative control were codon-optimized, synthesized and cloned into the mRNA production plasmid mRNAs were encapsulated with LNP (*49*). Briefly, mRNAs were transcribed to contain 101 nucleotide-long poly(A) tails. mRNAs were modified with m1Ψ-5′-triphosphate (TriLink #N-1081) instead of UTP and the *in vitro* transcribed mRNAs capped using the trinucleotide cap1 analog, CleanCap (TriLink #N-7413). mRNA was purified by cellulose (Sigma-Aldrich # 11363-250G) purification. All mRNAs were analyzed by agarose gel electrophoresis and were stored at -20°C. Cellulose-purified m1Ψ-containing RNAs were encapsulated in proprietary LNPs using a self-assembly process as previously described wherein an ethanolic lipid mixture of ionizable cationic lipid, phosphatidylcholine, cholesterol and polyethylene glycol-lipid was rapidly mixed with an aqueous solution containing mRNA at acidic pH. The RNA-loaded particles were characterized and subsequently stored at -80°C at a concentration of 1 mg/ml. The

mean hydrodynamic diameter of these mRNA-LNP was ~80 nm with a polydispersity index of 0.02-0.06 and an encapsulation efficiency of ~95%.

Animals, immunizations, and challenge viruses

Eleven-month-old female BALB/c mice were purchased from Envigo (#047) and were used for all experiments. The study was carried out in accordance with the recommendations for care and use of animals by the Office of Laboratory Animal Welfare (OLAW), National Institutes of Health and the Institutional Animal Care and Use Committee (IACUC) of University of North Carolina (UNC permit no. A-3410-01). mRNA-LNP vaccines were kept frozen until right before the vaccination. Mice were immunized with 1μg of each vaccine diluted in sterile 1XPBS in a 50μl volume and were given 25μl intramuscularly in each hind leg. Prime and boost immunizations were given three weeks apart. Three weeks post boost, mice were bled, sera was collected for analysis, and mice were moved into the BSL3 facility for challenge experiments. Animals were housed in groups of five and fed standard chow diets. Virus inoculations were performed under anesthesia and all efforts were made to minimize animal suffering. All mice were anesthetized and infected intranasally with 1×10^4 PFU/ml of SARS-CoV MA15, 1×10^4 PFU/ml of SARS-CoV-2 MA10, or 1×10^4 PFU/ml RsSHC014 which have been described previously (*9*, *34*, *50*). Mice were weighted daily and monitored for signs of clinical disease. Each challenge virus challenge experiment encompassed 50 mice with 10 mice per vaccine group to obtain statistical power.

Measurement of CoV spike binding by ELISA

A binding ELISA panel that included SARS-CoV spike Protein DeltaTM,

SARS-CoV-2 (2019-nCoV) spike Protein (S1+S2 ECD, His tag), MERS-CoV, Coronavirus spike S1+S2 (Baculovirus-Insect Cells, His), HKU1 (isolate N5) spike Protein (S1+S2 ECD, His Tag), OC43 spike Protein (S1+S2 ECD, His Tag), 229E spike Protein (S1+S2 ECD, His tag) Human coronavirus (HCoV-NL63) spike Protein (S1+S2 ECD, His Tag), Pangolin CoV_GXP4L_spikeEcto2P_3C8HtS2/293F, bat CoV RsSHC014_spikeEcto2P_3C8HtS2/293F, RaTG13_spikeEcto2P_3C8HtS2/293F, and bat CoV HKU3-1 spike were tested. Indirect binding ELISAs were conducted in 384 well ELISA plates (Costar #3700) coated with 2µg/ml antigen in 0.1M sodium bicarbonate overnight at 4°C, washed and blocked with assay diluent (1XPBS containing 4% (w/v) whey protein/ 15% Normal Goat Serum/ 0.5% Tween-20/ 0.05% Sodium Azide). Serum samples were incubated for 60 minutes in three-fold serial dilutions beginning at 1:30 followed by washing with PBS/0.1% Tween-20. HRP conjugated goat anti-mouse IgG secondary antibody (SouthernBiotech 1030-05) was diluted to 1:10,000 in assay diluent without azide, incubated at for 1 hour at room temperature, washed and detected with 20µl SureBlue Reserve (KPL 53-00-03) for 15 minutes. Reactions were stopped via the addition of 20µl HCL stop solution. Plates were read at 450nm. Area under the curve (AUC) measurements were determined from binding of serial dilutions.

ACE2 blocking ELISAs.

Plates were coated with 2µg/ml recombinant ACE2 protein, then washed and blocked with 3% BSA in PBS. While assay plates blocked, and sera was diluted 1:25 in 1%BSA/0.05% Tween-20. Then SARS-CoV-2 spike protein was mixed with equal volumes of each sample at a final spike concentration equal to the EC_{50} at which it binds to ACE2. The mixture was allowed to incubate at room temperature for 1 hour. Blocked assay plates were washed, and the serum-

spike mixture was added to the assay plates for a period of 1 hour at room temperature. Plates were washed and Strep-Tactin HRP, (IBA GmbH, Cat# 2-1502-001) was added at a dilution of 1:5000 followed by TMB substrate. The extent to which antibodies were able to block the binding of spike protein to ACE2 was determined by comparing the OD of antibody samples at 450nm to the OD of samples containing spike protein only with no antibody. The following formula was used to calculate percent blocking (100-(OD sample/OD of spike only) *100).

Measurement of neutralizing antibodies against live viruses

Full-length SARS-CoV-2 Seattle, SARS-CoV-2 D614G, SARS-CoV-2 B.1.351, SARS-CoV, WIV-1, and RsSHC014 viruses were designed to express nanoluciferase (nLuc) and were recovered via reverse genetics as described previously (*18*). Virus titers were measured in Vero E6 USAMRIID cells, as defined by plaque forming units (PFU) per ml, in a 6-well plate format in quadruplicate biological replicates for accuracy. For the 96-well neutralization assay, Vero E6 USAMRID cells were plated at 20,000 cells per well the day prior in clear bottom black walled plates. Cells were inspected to ensure confluency on the day of assay. Serum samples were tested at a starting dilution of 1:20 and were serially diluted 3-fold up to nine dilution spots. Serially diluted serum samples were mixed in equal volume with diluted virus. Antibody-virus and virus only mixtures were then incubated at 37°C with 5% CO_2 for one hour. Following incubation, serially diluted sera and virus only controls were added in duplicate to the cells at 75 PFU at 37°C with 5% CO_2. After 24 hours, cells were lysed, and luciferase activity was measured via Nano-Glo Luciferase Assay System (Promega) according to the manufacturer specifications. Luminescence was measured by a Spectramax M3 plate reader (Molecular Devices, San Jose,

CA). Virus neutralization titers were defined as the sample dilution at which a 50% reduction in RLU was observed relative to the average of the virus control wells.

Lung pathology scoring

Acute lung injury was quantified via two separate lung pathology scoring scales: Matute-Bello and Diffuse Alveolar Damage (DAD) scoring systems. Analyses and scoring were performed by a board vertified veterinary pathologist who was blinded to the treatment groups as described previously (*36*). Lung pathology slides were read and scored at 600X total magnification.

The lung injury scoring system used is from the American Thoracic Society (Matute-Bello) in order to help quantitate histological features of ALI observed in mouse models to relate this injury to human settings. In a blinded manner, three random fields of lung tissue were chosen and scored for the following: (A) neutrophils in the alveolar space (none = 0, 1–5 cells = 1, > 5 cells = 2), (B) neutrophils in the interstitial septa (none = 0, 1–5 cells = 1, > 5 cells = 2), (C) hyaline membranes (none = 0, one membrane = 1, > 1 membrane = 2), (D) Proteinaceous debris in air spaces (none = 0, one instance = 1, > 1 instance = 2), (E) alveolar septal thickening (< 2x mock thickness = 0, 2–4x mock thickness = 1, > 4x mock thickness = 2). To obtain a lung injury score per field, A–E scores were put into the following formula score = [(20x A) + (14 x B) + (7 x C) + (7 x D) + (2 x E)]/100. This formula contains multipliers that assign varying levels of importance for each phenotype of the disease state. The scores for the three fields per mouse were averaged to obtain a final score ranging from 0 to and including 1.

The second histology scoring scale to quantify acute lung injury was adopted from a lung pathology scoring system from lung RSV infection in mice (*37*). This lung histology scoring

scale measures diffuse alveolar damage (DAD). Similar to the implementation of the ATS histology scoring scale, three random fields of lung tissue were scored for the following in a blinded manner: 1= absence of cellular sloughing and necrosis, 2=Uncommon solitary cell sloughing and necrosis (1–2 foci/field), 3=multifocal (3+foci) cellular sloughing and necrosis with uncommon septal wall hyalinization, or 4=multifocal (>75% of field) cellular sloughing and necrosis with common and/or prominent hyaline membranes. The scores for the three fields per mouse were averaged to get a final DAD score per mouse. The microscope images were generated using an Olympus Bx43 light microscope and CellSense Entry v3.1 software.

Measurement of lung cytokines

Lung tissue was homogenized, spun down at 13,000g, and supernantant was used to measure lung cytokines using Mouse Cytokine 23-plex Assay (BioRad). Briefly, 50µl of lung homogenate supernatant was added to each well and the protocol was followed according to the manufacturer specifications. Plates were read using a MAGPIX multiplex reader (Luminex Corporation).

Biocontainment and biosafety

Studies were approved by the UNC Institutional Biosafety Committee approved by animal and experimental protocols in the Baric laboratory. All work described here was performed with approved standard operating procedures for SARS-CoV-2 in a biosafety level 3 (BSL-3) facility conforming to requirements recommended in the Microbiological and Biomedical Laboratories, by the U.S. Department of Health and Human Service, the U.S. Public

Health Service, and the U.S. Center for Disease Control and Prevention (CDC), and the National Institutes of Health (NIH).

Statistics

All statistical analyses were performed using GraphPad Prism 9. Statistical tests used in each figure are denoted in the corresponding figure legend.

REFERENCES AND NOTES

1. J. D. Cherry, P. Krogstad, SARS: The First Pandemic of the 21st Century. *Pediatric Research* **56**, 1-5 (2004).
2. A. M. Zaki, S. van Boheemen, T. M. Bestebroer, A. D. Osterhaus, R. A. Fouchier, Isolation of a novel coronavirus from a man with pneumonia in Saudi Arabia. *N Engl J Med* **367**, 1814-1820 (2012).
3. C. I. Paules, H. D. Marston, A. S. Fauci, Coronavirus Infections-More Than Just the Common Cold. *Jama* **323**, 707-708 (2020).
4. P. Zhou *et al.*, A pneumonia outbreak associated with a new coronavirus of probable bat origin. *Nature* **579**, 270-273 (2020).
5. The species Severe acute respiratory syndrome-related coronavirus: classifying 2019-nCoV and naming it SARS-CoV-2. *Nat Microbiol* **5**, 536-544 (2020).
6. P. Zhou, Z.-L. Shi, SARS-CoV-2 spillover events. *Science* **371**, 120-122 (2021).
7. P. Zhou *et al.*, Fatal swine acute diarrhoea syndrome caused by an HKU2-related coronavirus of bat origin. *Nature* **556**, 255-258 (2018).
8. C. E. Edwards *et al.*, Swine acute diarrhea syndrome coronavirus replication in primary human cells reveals potential susceptibility to infection. *Proc Natl Acad Sci U S A* **117**, 26915-26925 (2020).
9. V. D. Menachery *et al.*, A SARS-like cluster of circulating bat coronaviruses shows potential for human emergence. *Nat Med* **21**, 1508-1513 (2015).
10. V. D. Menachery *et al.*, SARS-like WIV1-CoV poised for human emergence. *Proc Natl Acad Sci U S A* **113**, 3048-3053 (2016).
11. W. Li *et al.*, Bats Are Natural Reservoirs of SARS-Like Coronaviruses. *Science* **310**, 676-679 (2005).
12. X. Y. Ge *et al.*, Isolation and characterization of a bat SARS-like coronavirus that uses the ACE2 receptor. *Nature* **503**, 535-538 (2013).
13. B. Hu *et al.*, Discovery of a rich gene pool of bat SARS-related coronaviruses provides new insights into the origin of SARS coronavirus. *PLoS Pathog* **13**, e1006698 (2017).
14. W. C. Koff, S. F. Berkley, A universal coronavirus vaccine. *Science* **371**, 759-759 (2021).
15. T. P. Sheahan *et al.*, Broad-spectrum antiviral GS-5734 inhibits both epidemic and zoonotic coronaviruses. *Sci Transl Med* **9**, (2017).
16. T. P. Sheahan *et al.*, An orally bioavailable broad-spectrum antiviral inhibits SARS-CoV-2 in human airway epithelial cell cultures and multiple coronaviruses in mice. *Sci Transl Med* **12**, (2020).
17. C. G. Rappazzo *et al.*, Broad and potent activity against SARS-like viruses by an engineered human monoclonal antibody. *Science* **371**, 823-829 (2021).
18. Y. J. Hou *et al.*, SARS-CoV-2 Reverse Genetics Reveals a Variable Infection Gradient in the Respiratory Tract. *Cell*.
19. A. A. Cohen *et al.*, Mosaic nanoparticles elicit cross-reactive immune responses to zoonotic coronaviruses in mice. *Science*, eabf6840 (2021).
20. Y. Honda-Okubo *et al.*, Severe acute respiratory syndrome-associated coronavirus vaccines formulated with delta inulin adjuvants provide enhanced protection while ameliorating lung eosinophilic immunopathology. *J Virol* **89**, 2995-3007 (2015).

21. M. Bolles *et al.*, A double-inactivated severe acute respiratory syndrome coronavirus vaccine provides incomplete protection in mice and induces increased eosinophilic proinflammatory pulmonary response upon challenge. *J Virol* **85**, 12201-12215 (2011).
22. L. Premkumar *et al.*, The receptor binding domain of the viral spike protein is an immunodominant and highly specific target of antibodies in SARS-CoV-2 patients. *Sci Immunol* **5**, (2020).
23. L. Liu *et al.*, Potent neutralizing antibodies against multiple epitopes on SARS-CoV-2 spike. *Nature* **584**, 450-456 (2020).
24. L. Dai *et al.*, A Universal Design of Betacoronavirus Vaccines against COVID-19, MERS, and SARS. *Cell* **182**, 722-733.e711 (2020).
25. D. Li *et al.*, The functions of SARS-CoV-2 neutralizing and infection-enhancing antibodies in vitro and in mice and nonhuman primates. *bioRxiv*, (2021).
26. X. Chi *et al.*, A neutralizing human antibody binds to the N-terminal domain of the Spike protein of SARS-CoV-2. *Science* **369**, 650-655 (2020).
27. N. Wang *et al.*, Structural Definition of a Neutralization-Sensitive Epitope on the MERS-CoV S1-NTD. *Cell Rep* **28**, 3395-3405.e3396 (2019).
28. N. Suryadevara *et al.*, Neutralizing and protective human monoclonal antibodies recognizing the N-terminal domain of the SARS-CoV-2 spike protein. *bioRxiv*, (2021).
29. M. M. Becker *et al.*, Synthetic recombinant bat SARS-like coronavirus is infectious in cultured cells and in mice. *Proc Natl Acad Sci U S A* **105**, 19944-19949 (2008).
30. D. Laczkó *et al.*, A Single Immunization with Nucleoside-Modified mRNA Vaccines Elicits Strong Cellular and Humoral Immune Responses against SARS-CoV-2 in Mice. *Immunity* **53**, 724-732.e727 (2020).
31. S. Awasthi *et al.*, Nucleoside-modified mRNA encoding HSV-2 glycoproteins C, D, and E prevents clinical and subclinical genital herpes. *Sci Immunol* **4**, (2019).
32. K. P. Egan *et al.*, An HSV-2 nucleoside-modified mRNA genital herpes vaccine containing glycoproteins gC, gD, and gE protects mice against HSV-1 genital lesions and latent infection. *PLoS Pathog* **16**, e1008795 (2020).
33. P. C. LaTourette, 2nd *et al.*, Protection against herpes simplex virus type 2 infection in a neonatal murine model using a trivalent nucleoside-modified mRNA in lipid nanoparticle vaccine. *Vaccine* **38**, 7409-7413 (2020).
34. S. R. Leist *et al.*, A Mouse-Adapted SARS-CoV-2 Induces Acute Lung Injury and Mortality in Standard Laboratory Mice. *Cell* **183**, 1070-1085.e1012 (2020).
35. G. Matute-Bello *et al.*, An official American Thoracic Society workshop report: features and measurements of experimental acute lung injury in animals. *Am J Respir Cell Mol Biol* **44**, 725-738 (2011).
36. T. P. Sheahan *et al.*, Comparative therapeutic efficacy of remdesivir and combination lopinavir, ritonavir, and interferon beta against MERS-CoV. *Nature Communications* **11**, 222 (2020).
37. M. E. Schmidt *et al.*, Memory CD8 T cells mediate severe immunopathology following respiratory syncytial virus infection. *PLoS Pathog* **14**, e1006810 (2018).
38. K. S. Corbett *et al.*, SARS-CoV-2 mRNA vaccine design enabled by prototype pathogen preparedness. *Nature*, (2020).
39. K. S. Corbett *et al.*, Evaluation of the mRNA-1273 Vaccine against SARS-CoV-2 in Nonhuman Primates. *N Engl J Med*, (2020).

40. K. Wu *et al.*, Serum Neutralizing Activity Elicited by mRNA-1273 Vaccine — Preliminary Report. *New England Journal of Medicine*, (2021).
41. L. A. Jackson *et al.*, An mRNA Vaccine against SARS-CoV-2 — Preliminary Report. *New England Journal of Medicine* **383**, 1920-1931 (2020).
42. E. E. Walsh *et al.*, Safety and Immunogenicity of Two RNA-Based Covid-19 Vaccine Candidates. *New England Journal of Medicine* **383**, 2439-2450 (2020).
43. L. R. Baden *et al.*, Efficacy and Safety of the mRNA-1273 SARS-CoV-2 Vaccine. *N Engl J Med*, (2020).
44. E. J. Anderson *et al.*, Safety and Immunogenicity of SARS-CoV-2 mRNA-1273 Vaccine in Older Adults. *N Engl J Med* **383**, 2427-2438 (2020).
45. K. O. Saunders *et al.*, SARS-CoV-2 vaccination induces neutralizing antibodies against pandemic and pre-emergent SARS-related coronaviruses in monkeys. *bioRxiv*, (2021).
46. N. B. Mercado *et al.*, Single-shot Ad26 vaccine protects against SARS-CoV-2 in rhesus macaques. *Nature*, (2020).
47. L. R. Banner, J. G. Keck, M. M. Lai, A clustering of RNA recombination sites adjacent to a hypervariable region of the peplomer gene of murine coronavirus. *Virology* **175**, 548-555 (1990).
48. J. G. Keck, L. H. Soe, S. Makino, S. A. Stohlman, M. M. Lai, RNA recombination of murine coronaviruses: recombination between fusion-positive mouse hepatitis virus A59 and fusion-negative mouse hepatitis virus 2. *J Virol* **62**, 1989-1998 (1988).
49. A. W. Freyn *et al.*, A Multi-Targeting, Nucleoside-Modified mRNA Influenza Virus Vaccine Provides Broad Protection in Mice. *Mol Ther* **28**, 1569-1584 (2020).
50. A. Roberts *et al.*, A mouse-adapted SARS-coronavirus causes disease and mortality in BALB/c mice. *PLoS Pathog* **3**, e5 (2007).

ACKNOWLEDGEMENTS

Funding: David R. Martinez is currently supported by a Burroughs Wellcome Fund Postdoctoral Enrichment Program Award and a Hanna H. Gray Fellowship from the Howard Hugues Medical Institute and was supported by an NIH NIAID T32 AI007151 and an NIAID F32 AI152296. This project was supported by the North Carolina Policy Collaboratory at the University of North Carolina at Chapel Hill with funding from the North Carolina Coronavirus Relief Fund established and appropriated by the North Carolina General Assembly. This project was funded in part by the National Institute of Allergy and Infectious Diseases, NIH, U.S. Department of Health and Human Services award 1U19 AI142759 (Antiviral Drug Discovery and Development Center awarded to R.S.B), 5R01AI132178 (partnership grant awarded to R.S.B), AI100625, and AI108197 to R.S.B., AI124429 and a BioNTech SRA to D.W., and E.A.V., as well as an animal models contract from the NIH (HHSN272201700036I) and U54CA260543 sponsored by NCI. Animal histopathology services were performed by the Animal Histopathology & Laboratory Medicine Core at the University of North Carolina, which is supported in part by an NCI Center Core Support Grant (5P30CA016086-41) to the UNC Lineberger Comprehensive Cancer Center.

Author contributions: Conceived the study: D.R.M. and R.S.B. designed experiments: D.R.M, R.S.B., performed laboratory experiments: D.R.M, A.S., S.R.L., A.W.; Provided critical reagents: K.O.S. Analyzed data and provided critical insight: D.R.M, A.S., S.R.L., G.D.l.C., A.W., E.A.V., R.P., M.B, D.L., B.Y., K.O.S., D.W., B.F.H., S.M.; Wrote the first draft of the paper: D.R.M; Read and edited the paper: D.R.M, A.S., S.R.L., G.D.l.C., A.W., E.A.V., R.P., M.B, D.L., B.Y., K.O.S., D.W., B.F.H., S.M., R.S.B. Funding acquisition: D.R.M., R.S.B. All authors reviewed and approved the manuscript. **Competing interests:** The University of North Carolina at Chapel Hill has filed provisional patents for which D.R.M. and R.S.B are co-

664 inventors (U.S. Provisional Application No. 63/106,247 filed on October 27th, 2020) for the
665 chimeric vaccine constructs and their applications described in this study.
666
667
668
669
670
671
672
673
674
675
676
677
678
679
680
681
682
683
684
685
686

687 **Figures**

688 **Figure 1. Genetic relationships among sarbecoviruses and mouse mRNA-LNP vaccination**
689 **strategy.** (**A**) Genetic diversity of pandemic and bat zoonotic coronaviruses. SARS-CoV is
690 shown in light blue, RsSHC014 is shown in purple, and SARS-CoV-2 is shown in red. (**B**)
691 Mouse vaccination strategy using mRNA-LNPs: group 1 received chimeric spike 1, 2, 3, and 4
692 as the prime and boost, group 2 received chimeric spike 1, 2 as the prime and chimeric spikes 3
693 and 4 as the boost, group 3 received chimeric spike 4 as the prime and boost, group 4 received
694 SARS-CoV-2 furin KO prime and boost, and group 5 received a norovirus capsid prime and
695 boost. Different vaccine groups were separately challenged with SARS-CoV, SARS-CoV-2, and
696 RsSHC014.

697

698 **Figure 2. Human pathogenic coronavirus spike binding and hACE2-blocking responses in**
699 **chimeric and monovalent SARS-CoV-2 spike-vaccinated mice.** ELISA binding responses in
700 the five different vaccination groups. Both pre-immunization and post-boost binding responses
701 were evaluated against sarbecovirus, MERS-CoV, and common-cold CoV antigens including:
702 (**A**) SARS-CoV Toronto Canada (Tor2) S2P, (**B**) SARS-CoV-2 S2P D614G, (**C**) SARS-CoV-2
703 RBD, (**D**) SARS-CoV-2 NTD, (**E**) Pangolin GXP4L spike, (**F**) RaTG13 spike, (**G**) RsSHC014
704 S2P spike, (**H**) HKU3-1 spike, (**I**) MERS-CoV spike, (**J**) hACE2 blocking responses against
705 SARS-CoV-2 spike in the distinct immunization groups. Blue squares represent mice from group
706 1, orange triangles represent mice from group 2, green triangles represent mice from group 3, red
707 rhombuses represent mice from group 4, and upside-down triangle represent mice from group 5.
708 Statistical significance for the binding and blocking responses is reported from a Kruskal-Wallis

709 test after Dunnett's multiple comparison correction. $^{*}p < 0.05$, $^{**}p < 0.01$, $^{***}p < 0.001$, and
710 $^{****}p < 0.0001$.
711
712
713 **Figure 3. Live sarbecovirus neutralizing antibody responses.** Neutralizing antibody responses
714 in mice from the five different vaccination groups against nanoluciferase-expressing infectious
715 molecular clones. (**A**) SARS-CoV neutralizing antibody responses from baseline and post boost
716 in the distinct vaccine groups. (**B**) SARS-CoV-2 neutralizing antibody responses from baseline
717 and post boost. (**C**) RsSHC014 neutralizing antibody responses from baseline and post boost. (**D**)
718 WIV-1 neutralizing antibody responses from baseline and post boost. (**E**) SARS-CoV-2 D614G
719 and South African B.1.351 variant of concern neutralizing activity in groups 1 and 4. (**F**)
720 Neutralization comparison of SARS-CoV-2 D614G vs. South African B.1.351. Statistical
721 significance for the live-virus neutralizing antibody responses is reported from a Kruskal-Wallis
722 test after Dunnett's multiple comparison correction. $^{*}p < 0.05$, $^{**}p < 0.01$, $^{***}p < 0.001$, and
723 $^{****}p < 0.0001$.
724
725 **Figure 4. *In vivo* protection against sarbecovirus challenge by chimeric spikes mRNA-**
726 **vaccines.** (**A**) Percent starting weight from the different vaccine groups of mice challenged with
727 SARS-CoV MA15. (**B**) SARS-CoV MA15 lung viral titers in mice from the distinct vaccine
728 groups. (**C**) SARS-CoV MA15 nasal turbinate titers. (**D**) Percent starting weight from the
729 different vaccine groups of mice challenged with SARS-CoV-2 MA10. (**E**) SARS-CoV-2 MA10
730 lung viral titers in mice from the distinct vaccine groups. (**F**) SARS-CoV-2 MA10 nasal
731 turbinate titers. Figure legend at the bottom right depicts the vaccines utilized in the different

groups. Statistical significance for weight loss is reported from a two-way ANOVA after Dunnett's multiple comparison correction. For lung and nasal turbinate titers, statistical significance is reported from a one-way ANOVA after Tukey's multiple comparison correction. $^{*}p < 0.05$, $^{**}p < 0.01$, $^{***}p < 0.001$, and $^{****}p < 0.0001$.

Figure 5. Lung pathology in protected vs. infected mice challenged with SARS-CoV and SARS-CoV-2. (**A**) Hematoxylin and eosin 4 days post infection lung analysis of SARS-CoV MA15 challenged mice from the different groups: group 1: chimeras 1-4 prime and boost, group 2: chimeras 1-2 prime and 3-4, group 3: chimera 4 prime and boost, SARS-CoV-2 furin KO prime and boost, and norovirus capsid prime and boost. (**B**) Lung pathology quantitation in SARS-CoV MA15 challenged mice from the different groups. Macroscopic lung discoloration score, microscopic acute lung injury (ALI) score, and diffuse alveolar damage (DAD) in day 4 post infection lung tissues are shown. (**C**) Hematoxylin and eosin 4 days post infection lung analysis of SARS-CoV-2 MA10 challenged mice from the different groups: group 1: chimeras 1-4 prime and boost, group 2: chimeras 1-2 prime and 3-4, group 3: chimera 4 prime and boost, SARS-CoV-2 furin KO prime and boost, and norovirus capsid prime and boost. (**D**) Lung pathology measurements in SARS-CoV-2 MA10 challenged mice from the different groups. Macroscopic lung discoloration score, microscopic acute lung injury (ALI) score, and diffuse alveolar damage (DAD) in day 4 post infection lung tissues are shown. Statistical significance is reported from a one-way ANOVA after Dunnet's multiple comparison correction. $^{*}p < 0.05$, $^{**}p < 0.01$, $^{***}p < 0.001$, and $^{****}p < 0.0001$.

Supplemental figures

Figure S1. Chimeric spike constructs from sarbecoviruses. (**A**) Spike chimera 1 includes the NTD from HKU3-1, the RBD from SARS-CoV, and the rest of the spike from SARS-CoV-2. (**B**) Spike chimera 2 includes the RBD from SARS-CoV-2 and the NTD and S2 from SARS-CoV. (**C**) Spike chimera 3 includes the RBD from SARS-CoV and the NTD and S2 SARS-CoV-2. (**D**) Spike chimera 4 includes the RBD from RsSHC014 and the rest of the spike from SARS-CoV-2. (**E**) SARS-CoV-2 furin KO spike vaccine and (**F**) is the norovirus capsid vaccine. (**G**). Protein expression of chimeric spikes, SARS-CoV-2 furin KO, and norovirus mRNA vaccines. GAPDH was used as the loading control. (**H**) Nanoluciferase expression of RsSHC014/SARS-CoV-2 chimeric spike live viruses.

Figure S2. Human common-cold CoV ELISA binding responses in chimeric and monovalent SARS-CoV-2 spike mRNA-LNP-vaccinated mice. Pre-immunization and post boost binding to (**A**) HCoV-HKU1 spike, (**B**) HCoV-OC43 spike, (**C**) HCoV-229E spike, and (**D**) HCoV-NL63 spike. Statistical significance for the binding and blocking responses is reported from a Kruskal-Wallis test after Dunnett's multiple comparison correction. $^{*}p < 0.05$, $^{**}p < 0.01$, $^{***}p < 0.001$, and $^{****}p < 0.0001$.

Figure S3. Comparison of neutralizing antibody activity of CoV mRNA-LNP vaccines against sarbecoviruses. (**A**) Group 1 neutralizing antibody responses against SARS-CoV-2, SARS-CoV, RsSHC014, and WIV-1 and (**B**) fold-change of SARS-CoV, RsSHC014, and WIV-1 neutralizing antibodies relative to SARS-CoV-2. (**C**) Group 2 neutralizing antibody responses against SARS-CoV-2, SARS-CoV, RsSHC014, and WIV-1 and (**D**) fold-change of SARS-CoV,

RsSHC014, and WIV-1 neutralizing antibodies relative to SARS-CoV-2. (**E**) Group 3 neutralizing antibody responses against SARS-CoV-2, SARS-CoV, RsSHC014, and WIV-1 and (**F**) fold-change of SARS-CoV, RsSHC014, and WIV-1 neutralizing antibodies relative to SARS-CoV-2. (**G**) Group 4 neutralizing antibody responses against SARS-CoV-2, SARS-CoV, RsSHC014, and WIV-1 and (**H**) fold-change of SARS-CoV, RsSHC014, and WIV-1 neutralizing antibodies relative to SARS-CoV-2.

Figure S4. *In vivo* protection against BtCoV challenge by chimeric spikes mRNA-vaccines. (**A**) Percent starting weight from the different vaccine groups of mice challenged with RsSHC014. (**B**) RsSHC014 lung viral titers in mice from the distinct vaccine groups. (**C**) RsSHC014 nasal turbinate titers in mice from the different immunization groups. Statistical significance is reported from a one-way ANOVA after Tukey's multiple comparison correction. $^{*}p < 0.05$, $^{**}p < 0.01$, $^{***}p < 0.001$, and $^{****}p < 0.0001$.

Figure S5. Survival analysis of immunized mice challenged with sarbecoviruses. (**A**) Survival analysis from immunized mice infected with SARS-CoV MA15 and (**B**) SARS-CoV-2 MA10. Statistical significance is reported from a Mantel-Cox test.

Figure S6. Lung cytokine analysis in protected vs. sarbecovirus-infected vaccinated mice. CCL2, IL-1α, G-SCF, and CCL4 in (**A**) SARS-CoV-infected mice and in (**B**) SARS-CoV-2-infected mice. Statistical significance for the binding and blocking responses is reported from a Kruskal-Wallis test after Dunnett's multiple comparison correction. $^{*}p < 0.05$, $^{**}p < 0.01$, $^{***}p < 0.001$, and $^{****}p < 0.0001$.

Figure 1

A

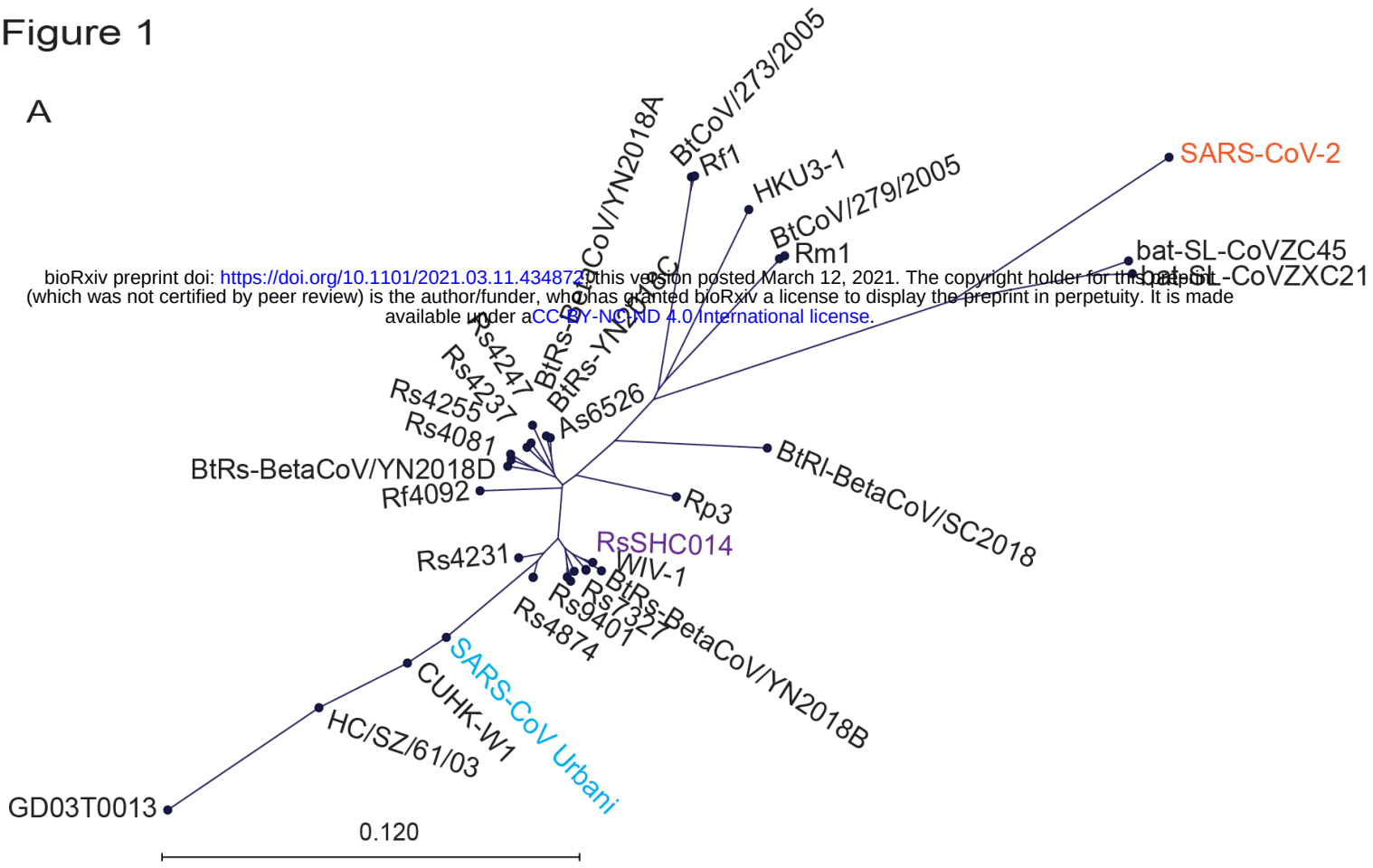

B

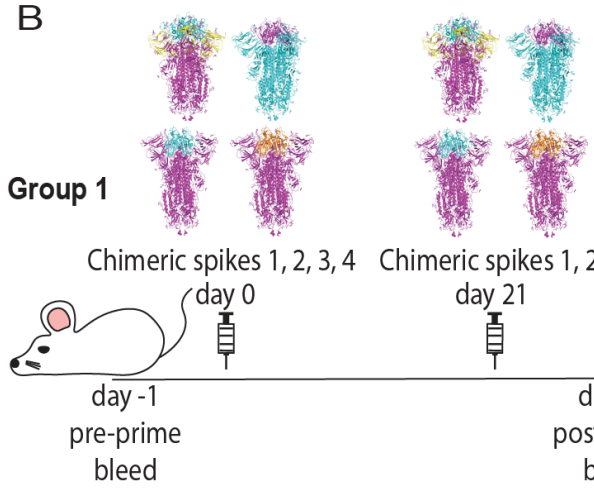

Figure 2

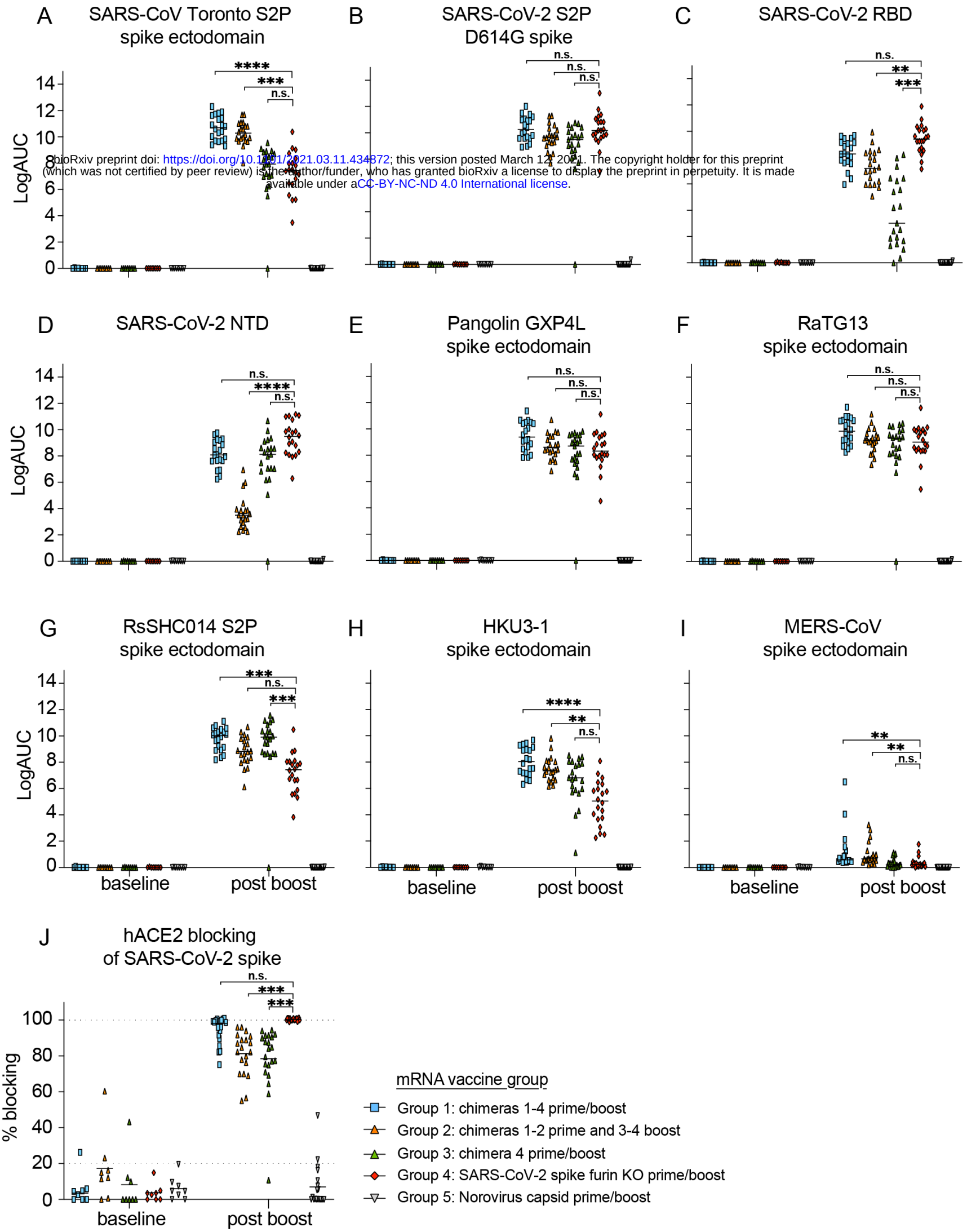

Figure 3

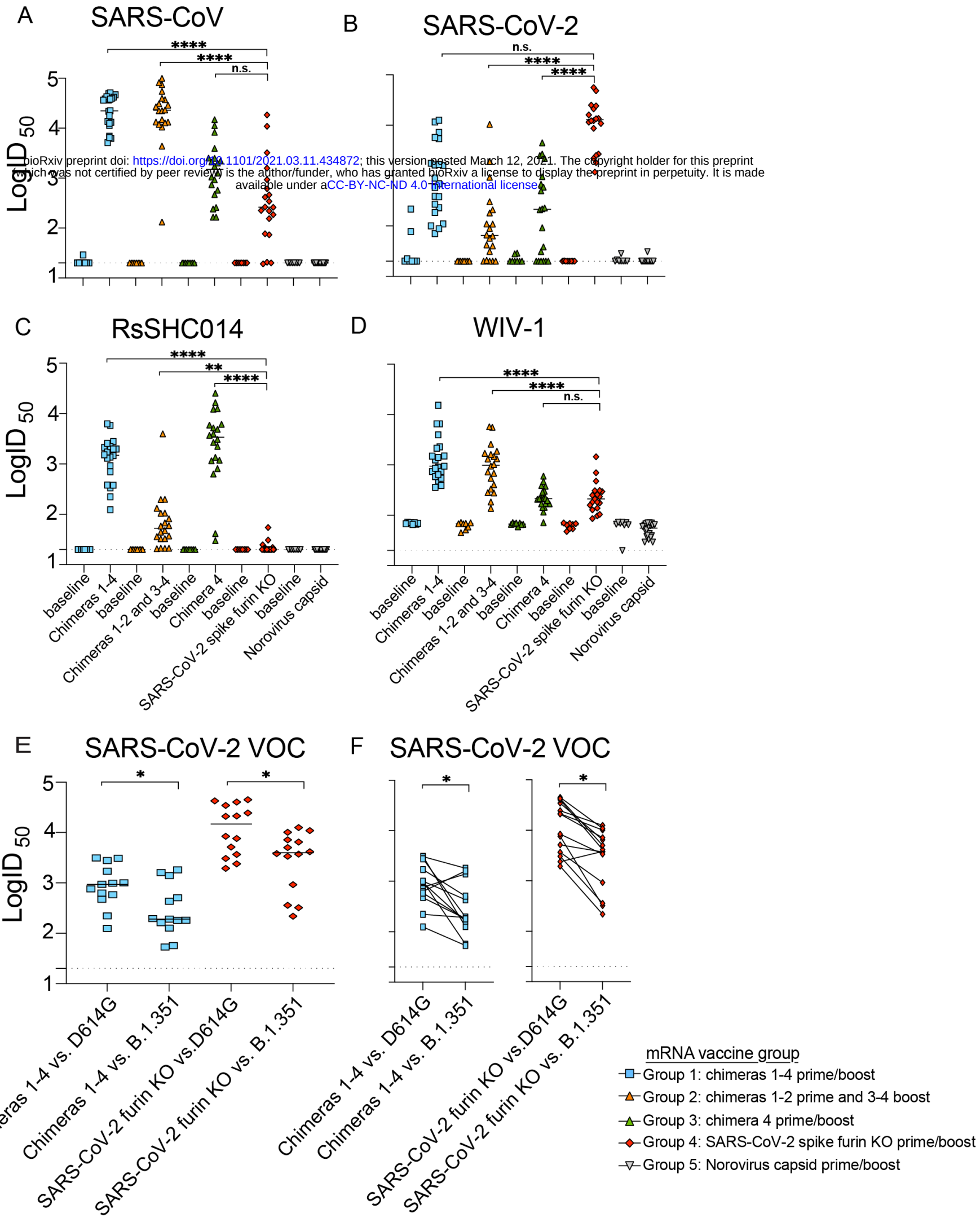

Figure 4

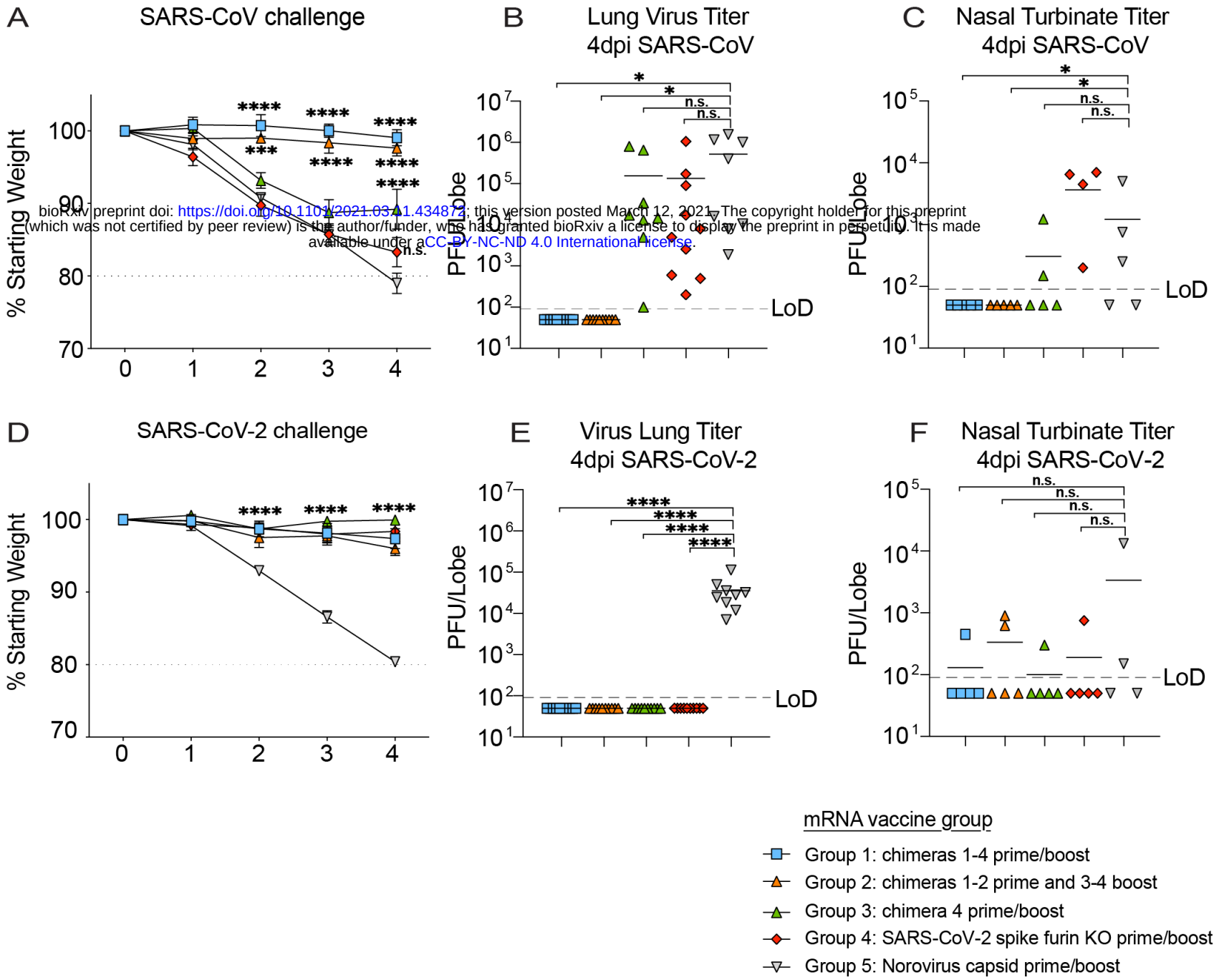

Figure 5

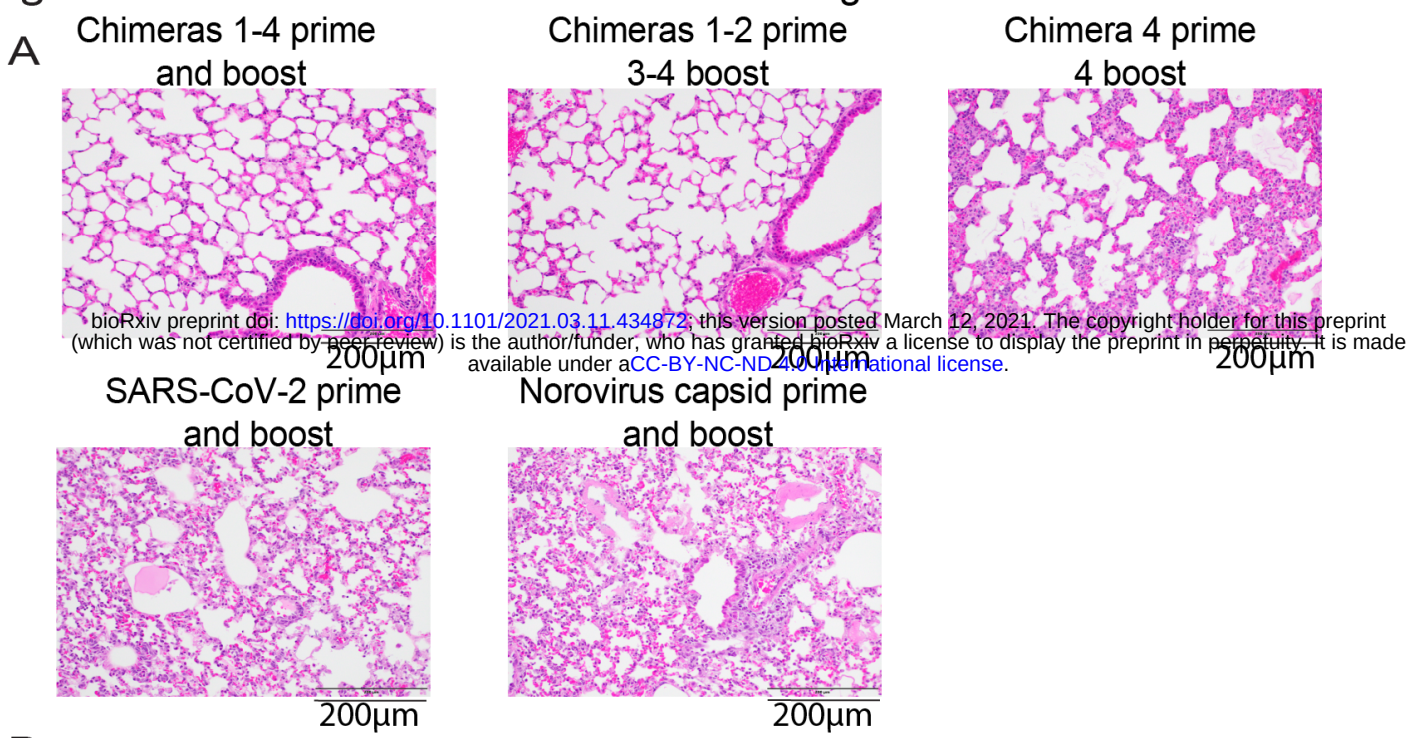

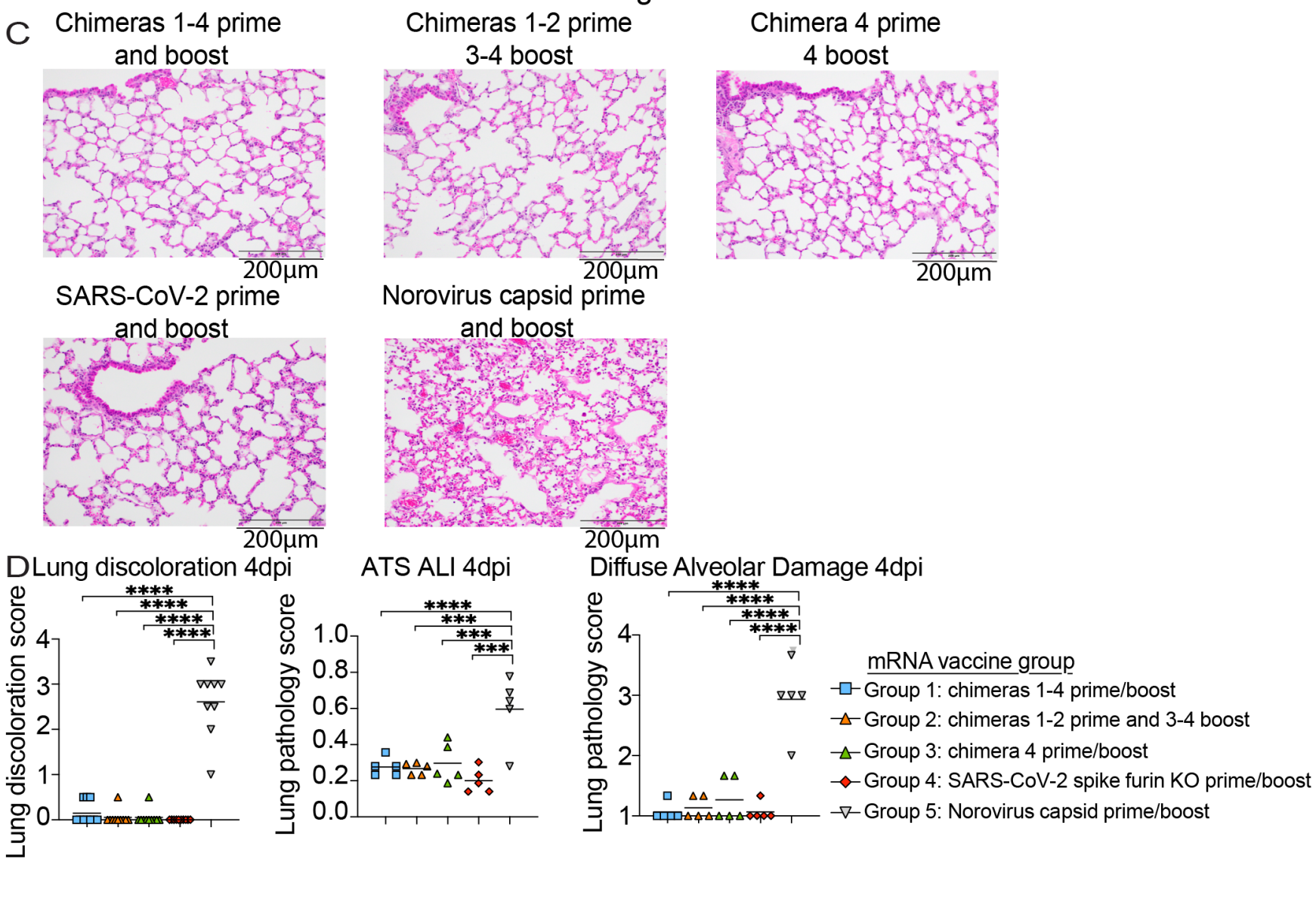

Figure S1

A Spike chimera 1
HKU3-1 NTD/SARS-CoV RBD/SARS-CoV2 S2

B Spike chimera 2
SARS-CoV-2 RBD/SARS-CoV S1 and S2

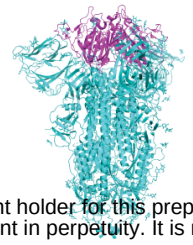

C Spike chimera 3
SARS-CoV RBD/SARS-CoV-2 S1 and S2

D Spike chimera 4
RsSHC014 RBD/SARS-CoV-2 S1 and S2

E SARS-CoV-2 wild type furin knockout

F Norovirus capsid

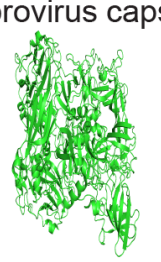

G

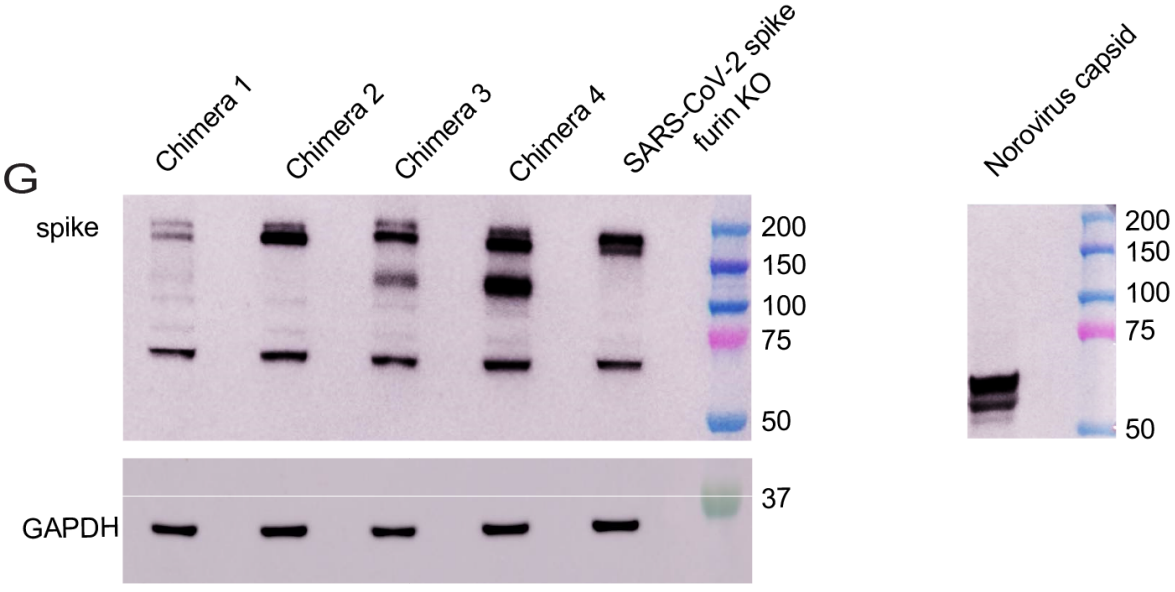

H Luciferase

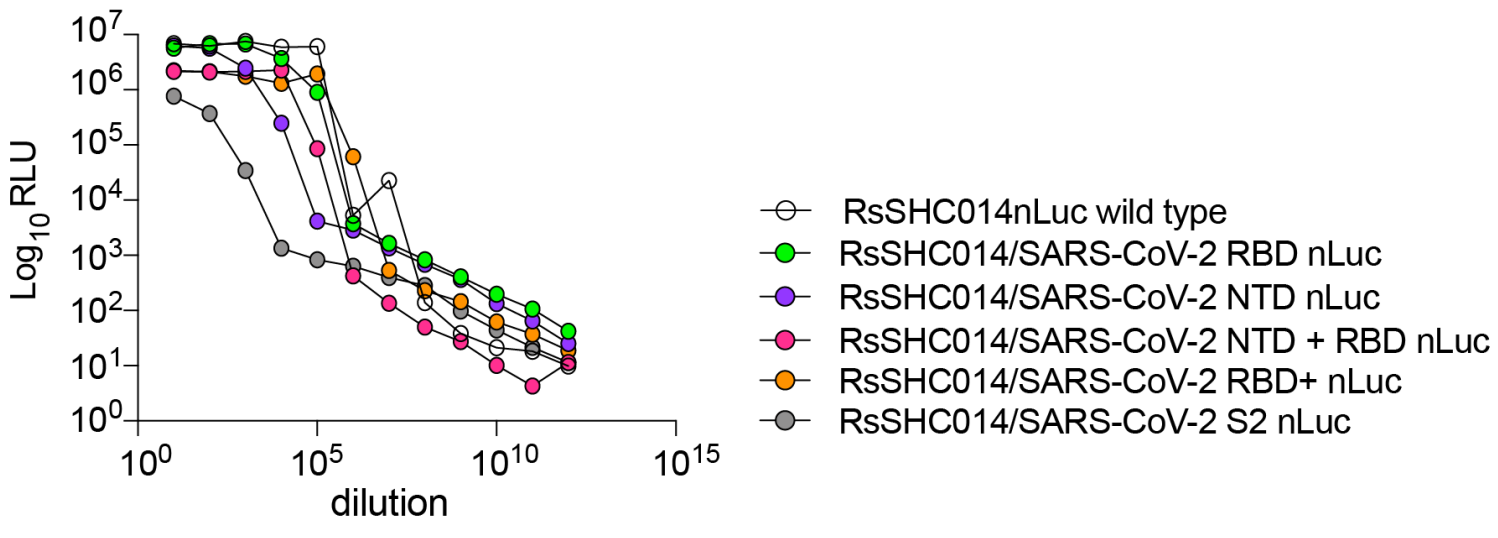

Figure S2

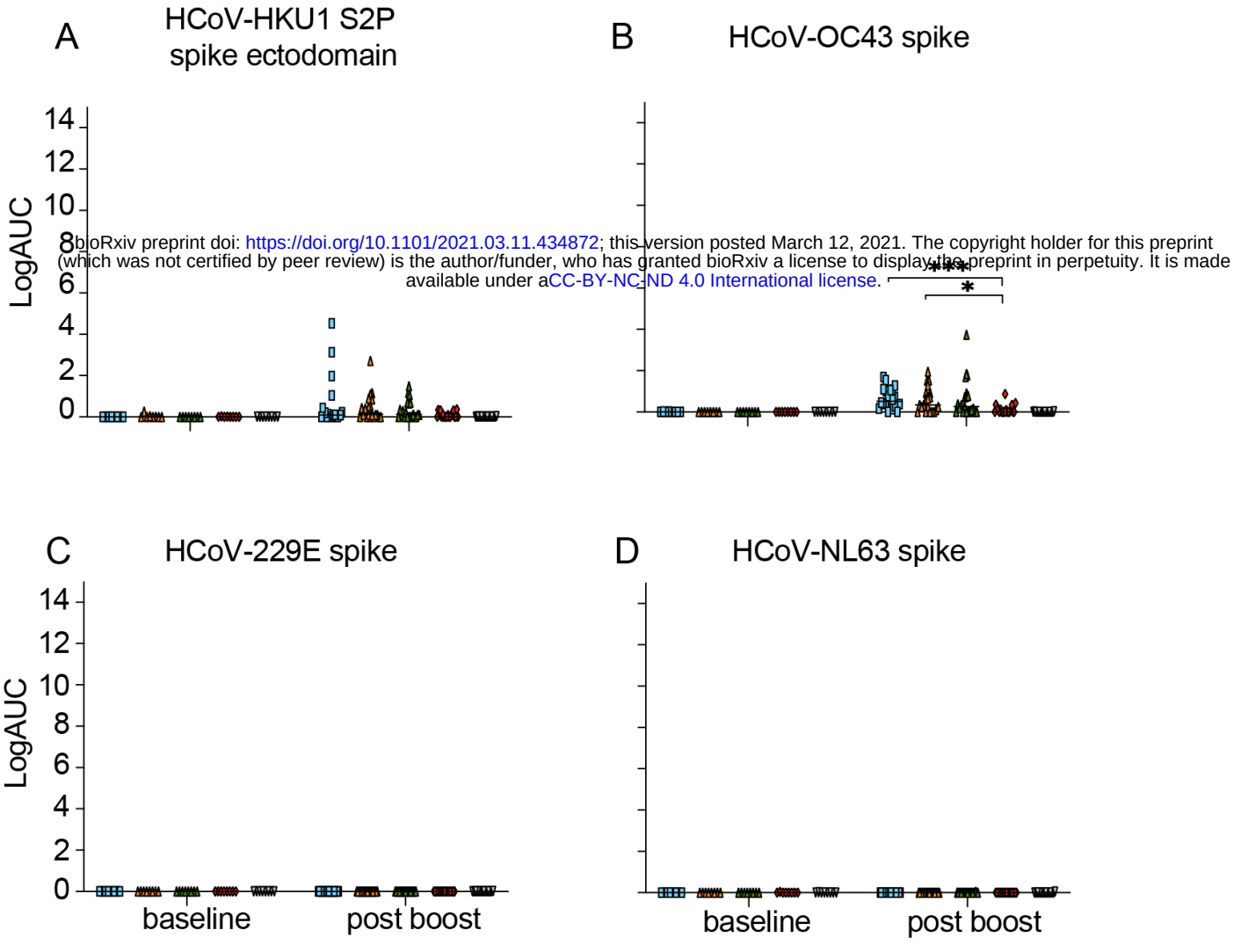

Figure S3

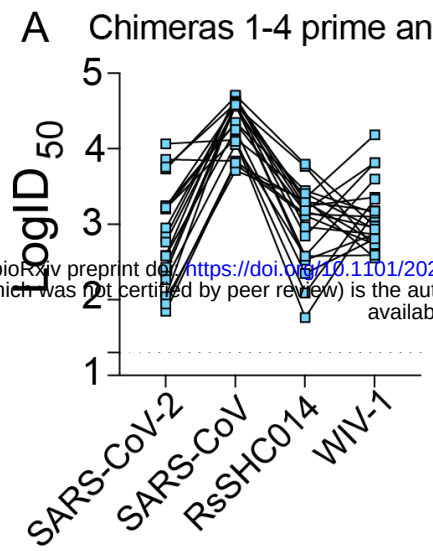

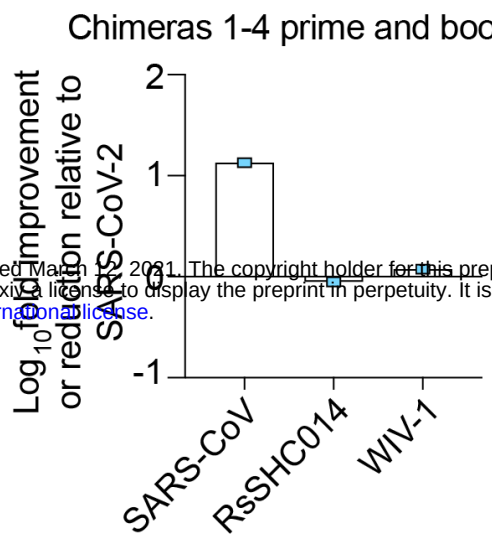

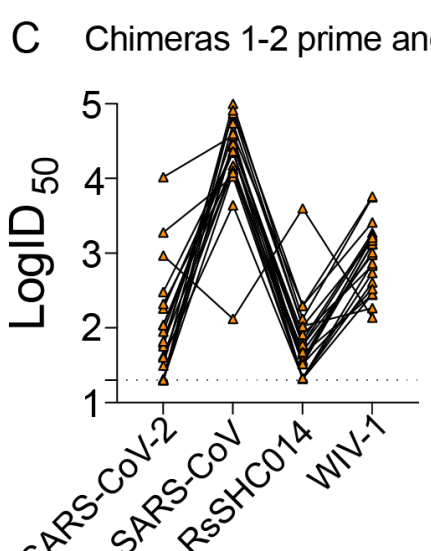

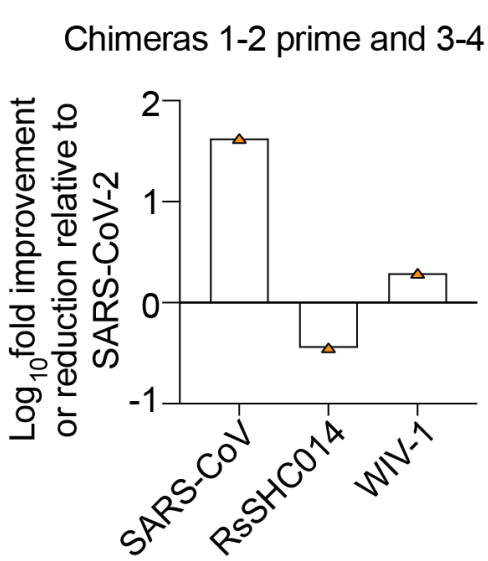

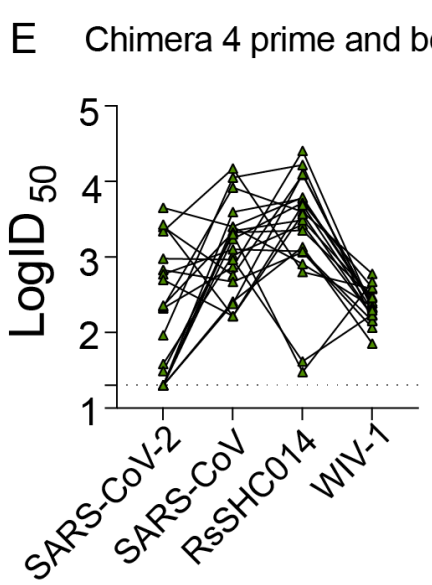

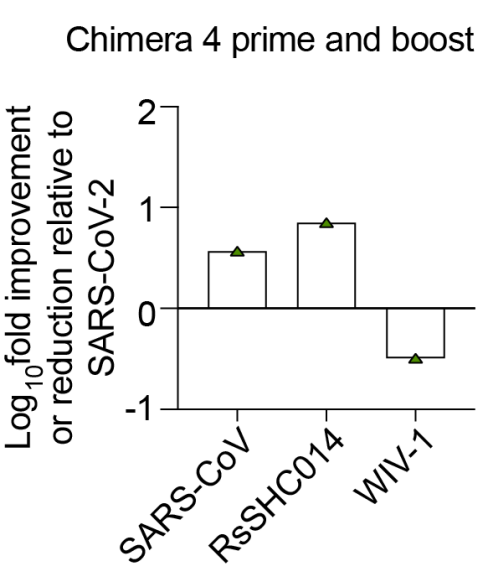

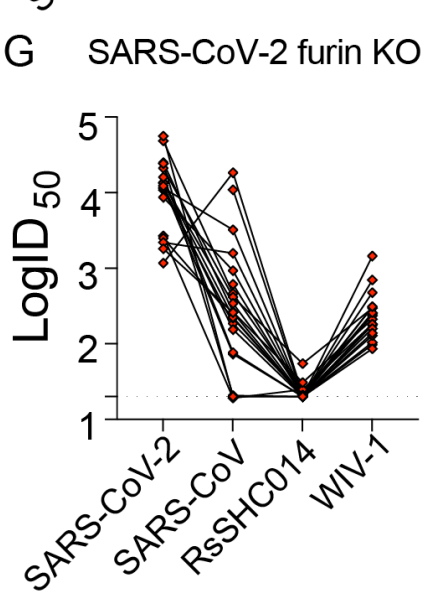

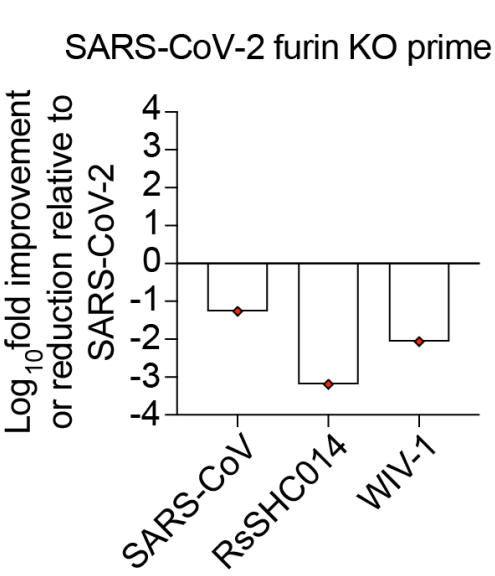

Figure S4

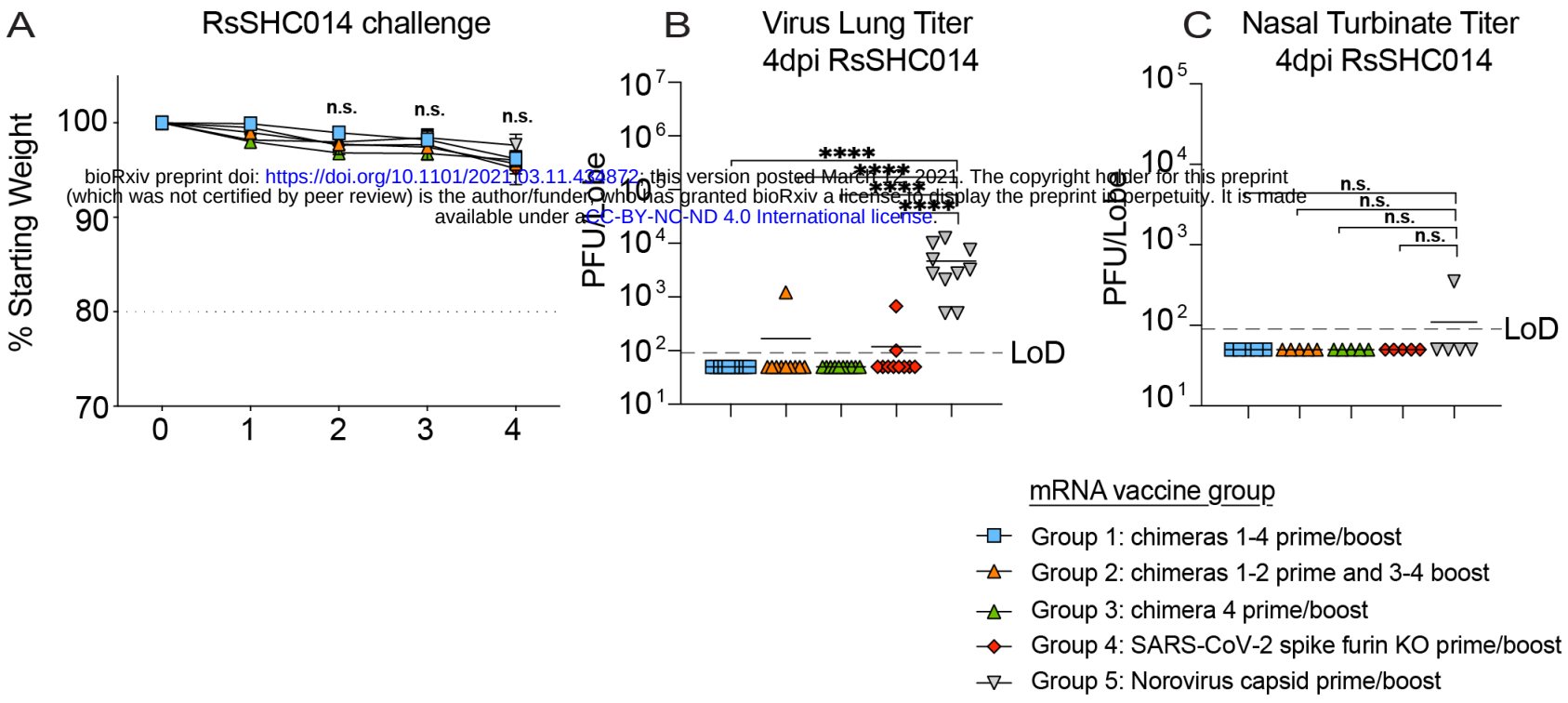

Figure S5

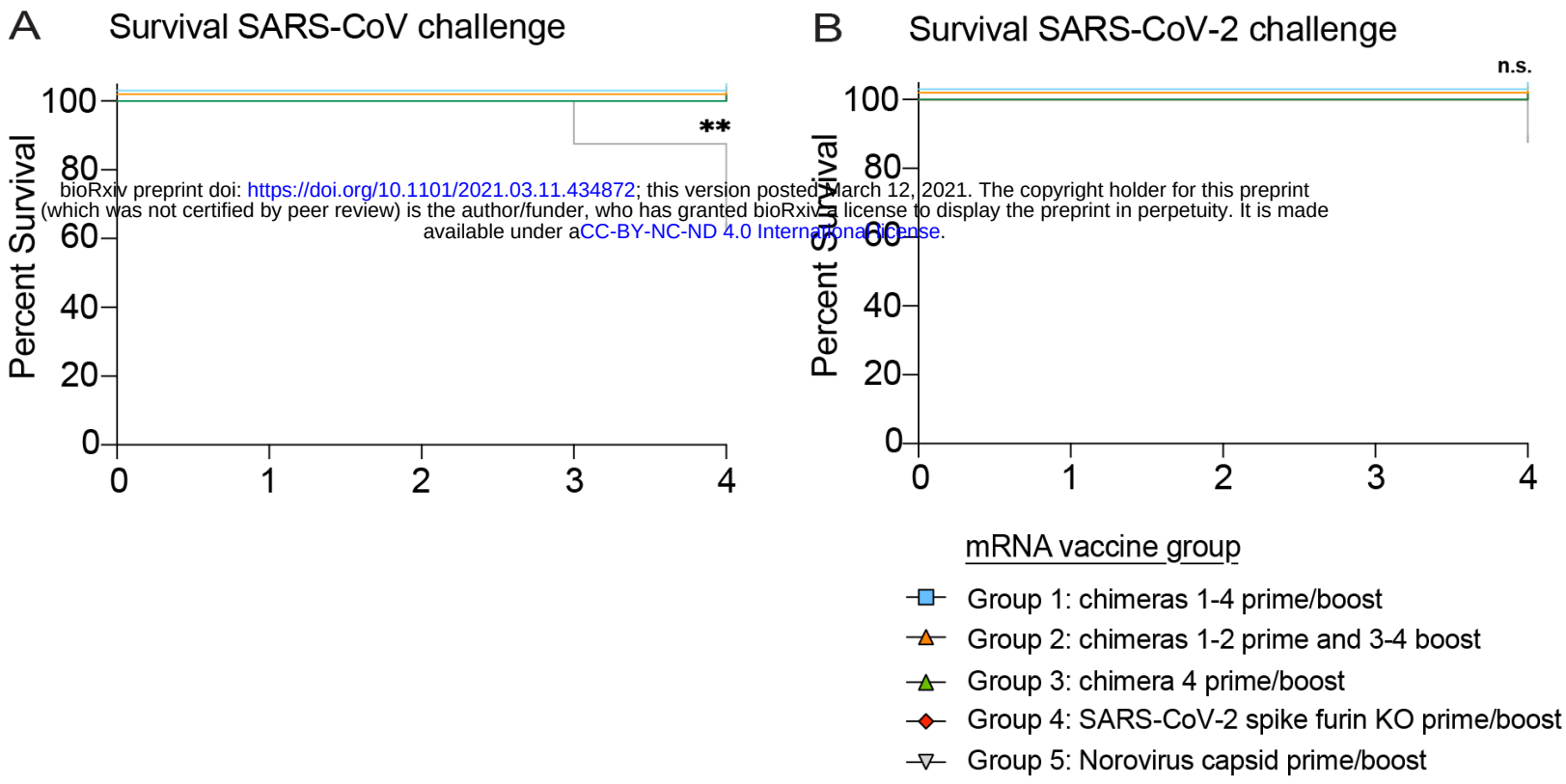

Figure S6